Time-irreversible Subconductance Gating Associated with Ba^{2+} Block of Large Conductance Ca^{2+}-activated K^+ Channels

Ricardo A. Bello and Karl L. Magleby

From the Department of Physiology and Biophysics, University of Miami School of Medicine, Miami, Florida 33101-6430

ABSTRACT Ba^{2+} block of large conductance Ca^{2+}-activated K^+ channels was studied in patches of membrane excised from cultures of rat skeletal muscle using the patch clamp technique. Under conditions in which a blocking Ba^{2+} ion would dissociate to the external solution (150 mM *N*-methyl-D-glucamine^+_o, 500 mM K^+_i, 10 μM Ba^{2+}_i, +30 mV, and 100 μM Ca^{2+}_i to fully activate the channel), Ba^{2+} blocks with a mean duration of ~2 s occurred, on average, once every ~100 ms of channel open time. Of these Ba^{2+} blocks, 78% terminated with a single step in the current to the fully open level and 22% terminated with a transition to a subconductance level at ~0.26 of the fully open level (preopening) before stepping to the fully open level. Only one apparent preclosing was observed in ~10,000 Ba^{2+} blocks. Thus, the preopenings represent Ba^{2+}-induced time-irreversible subconductance gating. The fraction of Ba^{2+} blocks terminating with a preopening and the duration of preopenings (exponentially distributed, mean = 0.75 ms) appeared independent of changes in $[Ba^{2+}]_i$ or membrane potential. The fractional conductance of the preopenings increased from 0.24 at +10 mV to 0.39 at +90 mV. In contrast, the average subconductance level during normal gating in the absence of Ba^{2+} was independent of membrane potential, suggesting different mechanisms for preopenings and normal subconductance levels. Preopenings were also observed with 10 mM Ba^{2+}_o and no added Ba^{2+}_i. Adding K^+, Rb^+, or Na^+ to the external solution decreased the fraction of Ba^{2+} blocks with preopenings, with K^+ and Rb^+ being more effective than Na^+. These results are consistent with models in which the blocking Ba^{2+} ion either induces a preopening gate, and then dissociates to the external solution, or moves to a site located on the external side of the Ba^{2+} blocking site and acts directly as the preopening gate.

KEY WORDS: barium block • skeletal muscle • microscopic reversibility • asymmetric gating • preopening

INTRODUCTION

Blocking ions have served as useful probes to gain insight into the structure of the conducting pores of K^+ channels (Armstrong, 1971, 1975; Armstrong et al., 1982; Yellen, 1984*a*, 1984*b*; Ferguson, 1991; Lucchesi and Moczydlowski, 1991; Slesinger et al., 1993; Taglialatela et al., 1993; Hurst et al., 1995; Sohma et al., 1996; Baukrowitz and Yellen, 1996). One blocking ion that has yielded a great deal of information about the pore of large conductance Ca^{2+}-activated K^+ (BK)[1] channels is Ba^{2+} (Vergara and Latorre, 1983; Benham et al., 1985; Miller, 1987; Miller et al., 1987; Neyton and Miller, 1988*a*, 1988*b*; Neyton and Pelleschi, 1991; Diaz et al., 1996). Ba^{2+} enters and blocks the pore of the open channel in a voltage-dependent manner from either side of the membrane, with much higher concentrations of Ba^{2+} required for the same blocking rate from the external as from the internal solution. Ba^{2+} typically remains bound to the blocking site, situated 30–50% through the electric field from the inside, for several seconds. Ba^{2+} then dissociates, restoring the current to the level observed before the block. With positive membrane potentials and the impermeant ion *N*-methyl-D-glucamine$^+$ (NMDG$^+$) replacing external K^+, Ba^{2+} typically dissociates to the outside solution. Adding external K^+, which can bind to external lock-in and enhancement sites, can force dissociation of the blocking Ba^+ to the internal solution (Neyton and Miller, 1988*a*, 1988*b*). From a series of experiments examining the effects of external and internal ions and membrane potential on the duration of Ba^+ blocks, Neyton and Miller (1988*b*) suggested that there are at least four K^+ binding sites within the pore of the BK channel that can be simultaneously occupied: an internal lock-in site located 30% through the electric field from the inside, an external enhancement site located 50% through the electric field, the Ba^+ blocking site located between the internal lock-in and the external enhancement sites, and an external lock-in site located 85% through the electric field from the inside.

The impetus for our study was the chance observation by Ferguson et al. (1994) that Ba^{2+} blockade may be more complex than detailed above. They found that, when all the external K^+ was replaced with

Address correspondence to Dr. Karl L. Magleby, Department of Physiology and Biophysics R-430, University of Miami School of Medicine, Miami, FL 33101-6430. Fax: 305-243-6898; E-mail: kmagleby@mednet.med.miami.edu

[1]*Abbreviations used in this paper:* BK channel, Ca^{2+}-activated K^+ channel; NMDA, *N*-methyl-D-glucamine.

$NMDG^+$, the transition of the current from the blocked level to the fully open level often passed through a subconductance level at ~25% of the fully open level before opening fully. The unblocking transition through the subconductance level was termed a preopening because it preceded the fully open level.

We now study further the preopenings to investigate their mechanism. We find that the preopenings represent time-irreversible subconductance gating, adding another interesting example to gating processes that violate microscopic reversibility (Hamill and Sakmann, 1981; Trautmann, 1982; Richard and Miller, 1990; Cull-Candy and Usowicz, 1987; Wyllie et al., 1996; Schneggenburger and Ascher, 1997). The preopenings are observed under experimental conditions that favor the dissociation of the blocking Ba^{2+} to the external solution (0 external K^+) and are not seen under conditions where the blocking Ba^{2+} ion dissociates to the internal solution (100 mM external K^+). The preopenings are found to have conductance properties that differ from the subconductance levels that occur during normal gating, suggesting different underlying mechanisms. Two models with irreversible steps are considered that appear consistent with the Ba^{2+}-induced time-irreversible subconductance gating. Preliminary reports of some of these results have appeared (Ferguson et al., 1994; Bello and Magleby, 1996).

METHODS

BK Channels from Primary Cultures of Rat Skeletal Muscle

Fetuses were removed from 19–21-d untimed pregnant Sprague-Dawley rats killed by CO_2 inhalation. Skeletal muscle from the hind- and forelimbs of the fetuses was minced with scalpels and enzymatically dissociated by stirring for 30 min at 37°C in DMEM (31600; Gibco Laboratories, Grand Island, NY) with 0.1 mg/ml trypsin (T8253; Sigma Chemical Co., St. Louis, MO) and 1 mg/ml collagenase (C9891; Sigma Chemical Co.). The resulting cell suspension was centrifuged at 1000 *g* for 15 min and the supernatant was discarded. The cells were resuspended in culture medium consisting of DMEM with 10% fetal bovine serum and 100 U/ml penicillin with 100 μg/ml streptomycin (P0781; Sigma Chemical Co.). The suspension was passed through a 30-μm nylon mesh to remove any undigested tissue and preplated for 30 min on a fibronectin-coated 60-mm tissue culture dish to reduce the number of fibroblasts. Cells were counted on a standard hemocytometer using trypan blue exclusion to determine viability and diluted to 300,000 cells/ml using the same medium as above. Cells were then plated using 1.5 ml of the diluted cell suspension per 35-mm tissue culture dish (Falcon 3001; Becton Dickinson & Co., Mountain View, CA). Cultures were maintained in a 90% air/10% CO_2 water-saturated atmosphere. After ~3–4 d in culture, the myoblasts fused to form myotubes. At this point, the culture medium was changed to a serum-free medium consisting of DMEM, 100 U/ml penicillin, 100 μg/ml streptomycin, 1 mg/ml bovine serum albumin (A8412), 50 μg/ml holo-transferrin (T1283), and 5 μg/ml insulin (I1882; all from Sigma Chemical Co.). The culture medium was replaced every 2 d thereafter with the serum-free medium. The cultured cells were suitable for patch clamping for 3–4 d after forming myotubes.

Single-Channel Recording and Solutions

Currents flowing through large conductance Ca^{2+}-activated K^+ channels in excised patches of surface membrane from the cultured rat myotubes were recorded using the inside-out patch clamp technique (Hamill et al., 1981). Currents were filtered at 10 kHz (−3 dB, four-pole low pass Bessel filter) using the internal filter in the Axopatch 200A amplifier (Axon Instruments, Foster City, CA), digitized using a VR-10B (Instrutech Corp., Great Neck, NY), and stored on video tape for subsequent analysis. BK channels were identified by their K^+ selectivity, large characteristic conductance, and activation by internal Ca^{2+} and depolarization (Barrett et al., 1982). Most experiments were performed on patches containing a single BK channel. However, a few experiments were also performed on patches containing two to three BK channels. With multichannel patches, only the segments of current records where a single channel was active (the others were blocked by Ba^{2+}) were analyzed.

Unless indicated otherwise, the solution at the normal intracellular side of the channel (internal) contained 500 mM KCl and 100–250 μM Ca^{2+}, and the external solution contained 150 mM NMDG-Cl. In addition, both solutions contained 5 mM TES (*N*-tris (hydroxymethyl)methyl-2-aminoethane sulfonic acid) buffer and the pH was adjusted to 7.0. The internal solution was changed by means of a gravity-fed perfusion system supplying a microchamber into which the tip of the patch pipette was placed (Barrett et al., 1982). The membrane potential was held at +30 mV unless otherwise indicated. Experiments were performed at room temperature (21–24°C).

Initial Analysis of the Single-Channel Current Records

Currents were sampled from tape by computer every 20 μs using a Digidata 1200 A/D converter (Axon Instruments, Foster City, CA) without additional filtering. A custom program using graphic commands (HP graphics language) was then used to print the current traces for the entire experiment on a laser printer at 10 s per trace and eight traces per page. These printouts were examined for artifacts, such as voltage spikes, that could interfere with the analysis. Another custom program allowed display and scrolling of the current records on the computer monitor (486 or Pentium) so that the occasional artifacts could be excluded from the data.

Detection of Ba^{2+} Blocks

After visually inspecting the current records, the program was used to measure the durations of the open and shut intervals from the previously examined current records using 50% threshold detection. For the few records obtained from patches containing more than one channel, the threshold was set to 50% of the open current level when only a single channel was active. Such an approach would not be suitable for detailed kinetic analysis, but was adequate for finding current transitions associated with Ba^{2+} blocking to the zero current level and Ba^{2+} unblocking from the zero current level. Since any one of the blocked channels could unblock in the few patches with multiple channels, the observed blocking durations were corrected to those that would be observed for a single channel by multiplying the observed duration by the number of channels in the patch. The plotted results on block duration in this paper were based on patches containing a single BK channel.

To identify the Ba^{2+} blocks, the shut dwell times were log binned at 25 bins/log unit and fitted with sums of exponential components (McManus et al., 1987; McManus and Magleby, 1988). Intervals with durations less than two dead times were excluded from the fitting. Ba^{2+} blocks were defined as the expo-

nential component of long shut intervals that became apparent in the experimental data with the addition of Ba^{2+}, as shown in Rothberg et al. (1996). In some experiments, a few apparent Ba^{2+} blocks were present in the absence of added Ba^{2+} due to the submicromolar concentration of Ba^{2+} that contaminates reagent grade KCl salts (Neyton and Miller, 1988*a*; Rothberg et al., 1996). In these experiments, Ba^{2+} blocks were defined as the component of long shut intervals whose area greatly increased with added Ba^{2+}. The contaminating Ba^{2+} in the solutions was estimated at <0.1 μM by comparing the apparent Ba^{2+} block rate in the absence of added Ba^{2+} to the rate with known amounts of added Ba^{2+}.

In the absence of Ba^{2+}, and at the high internal Ca^{2+} concentrations used in these experiments to fully activate the channel, the shut dwell-time distribution was typically fit by five to seven significant exponential components. The shut components with the longest mean durations in the absence of Ba^{2+} typically had time constants of 100–150 ms, consistent with the longest shut intervals typically observed when high concentrations of Ca^{2+} in the internal solution are used to activate the channel (Rothberg et al., 1996). The shut dwell-time distribution obtained after adding Ba^{2+} were found to be described by the same components as in the absence of Ba^{2+} plus an additional component with a much longer time constant typically in the range of 1–15 s.

Because of the exponential distribution of interval durations in the various components, there was overlap between the durations of intervals arising from Ba^{2+} block and those arising from normal gating. To maximize the probability that intervals defined as arising from Ba^{2+} blocks actually arose from Ba^{2+} blocks, the analysis was restricted to shut intervals longer than five times the time constant of the longest component in the absence of Ba^{2+}. With this restriction, typically $<10\%$ of the intervals designated as Ba^{2+} blocks would have arisen from normal gating components. An error of this magnitude would have little effect on the results.

Measuring the Amplitudes and Durations of Transitions to Subconductance Levels

The current record during the closing and opening transition of each identified Ba^{2+} block was automatically located and displayed at high time resolution. Each blocking and unblocking transition was then inspected visually for subconductance levels. If such a subconductance level was found, its amplitude and duration were measured by user-controlled cursor lines. An example of a display with cursor lines measuring the amplitude and duration of a subconductance transition (defined as a preopening in the RESULTS) is shown in Fig. 1. As evident in this figure and those figures in the RESULTS, transitions to the subconductance levels were typically unambiguous and could be clearly identified and measured. Since it can be difficult to distinguish between a brief duration subconductance level and a brief duration full opening whose amplitude would be reduced by the limited frequency response, only those subconductance levels lasting longer than 150 μs were included in the analysis.

RESULTS

Current Transitions Resulting from Unblocking of Ba^{2+} Can Be Associated with a Preopening Subconductance Level

Outward currents flowing through a single BK channel in an inside-out patch of surface membrane from cultured rat skeletal muscle are shown in Fig. 2 *A*, where a 144-s continuous record is broken into four segments

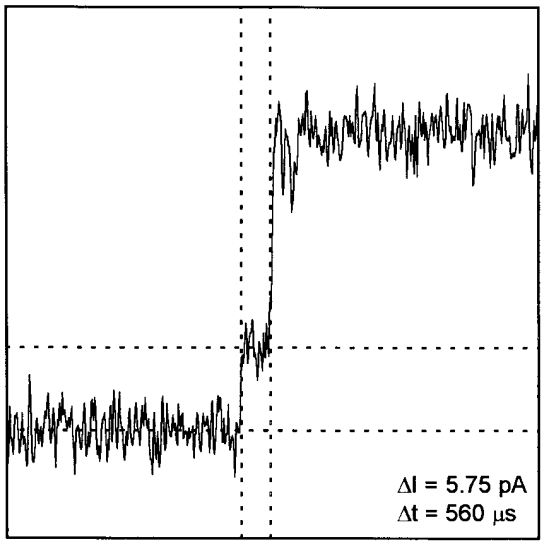

FIGURE 1. Computer display of a single channel current showing the setting of the cursor lines to measure the amplitude and duration of a preopening after a Ba^{2+} block.

for display. Under the conditions of this experiment with 500 mM internal KCl, 150 mM external NMDG-Cl (0 mM external K^+), and a holding potential of +30 mV, channel openings are indicated by outward (upward) currents. The large single channel current (~20 pA) under these conditions increased the ability to detect subconductance levels.

As described previously (Rothberg et al., 1996), currents recorded in the presence of high (100–250 μM) internal Ca^{2+} typically contained four or more types of activity: (*a*) normal gating, as indicated by long bursts of high activity; (*b*) gating in the low activity mode, consisting of a series of brief openings separated by long (mean of 100 ms) shut intervals; (*c*) isolated long (mean of 127 ms) shut intervals; and (*d*) an occasional shut interval of several seconds duration due to Ba^{2+} block arising from the submicromolar contaminating Ba^{2+} in the reagent grade KCl (Neyton and Miller, 1988*a*).

Fig. 2 *B* shows a 144-s current record from the same patch after Ba^{2+}, a potent blocker of many K^+ channels (Armstrong et al., 1982; Vergara and Latorre, 1983; Miller et al., 1987) is added to the internal solution at a concentration of 10 μM. Just as described previously (Vergara and Latorre, 1983), Ba^{2+} introduced long shut intervals, consistent with slow Ba^{2+} blockade of the channel. The apparent Ba^{2+} blocks were identified from analysis of the distributions of all shut intervals in the presence and absence of internal Ba^{2+}, as described in METHODS. The mean duration of the Ba^{2+} blocks for the entire 412-s record for the experiment presented in Fig. 2 *B* was 1.4 s.

High internal Ca^{2+} was used in the experiments to make the durations of the shut intervals associated with

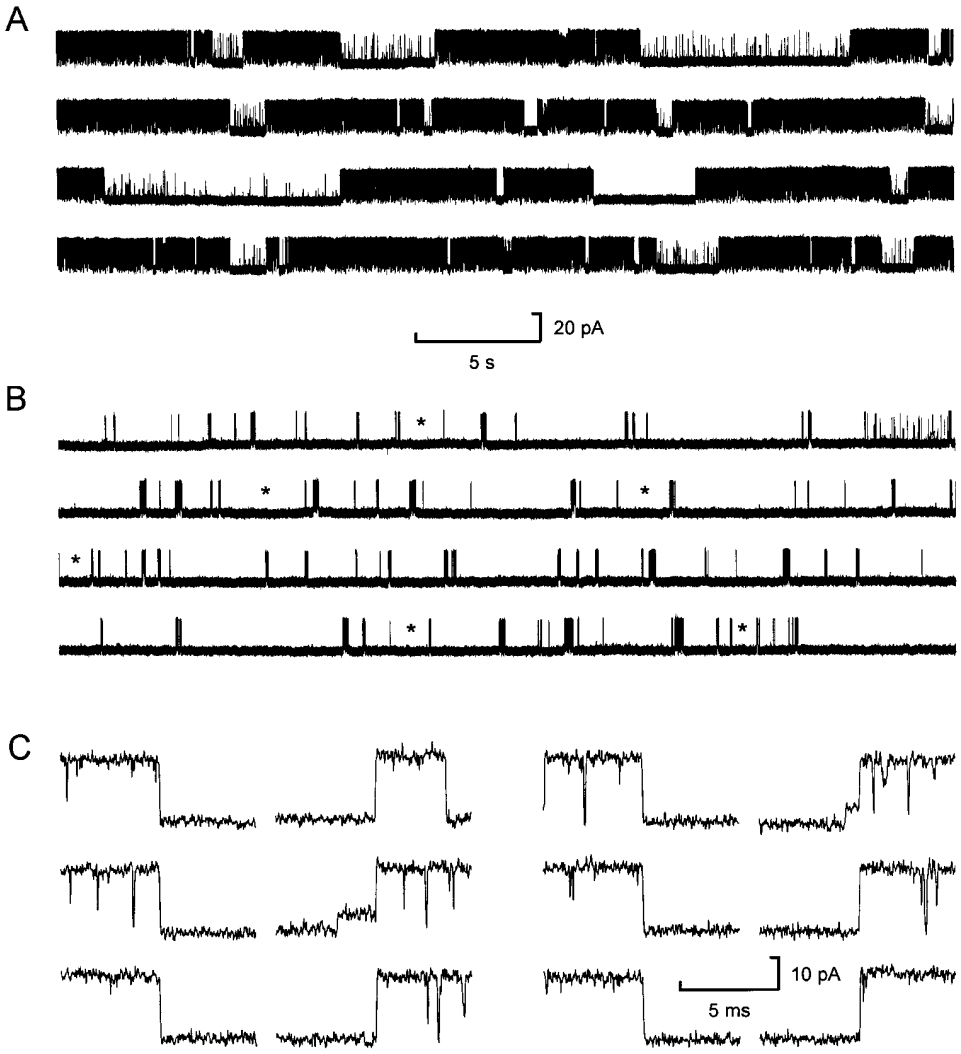

FIGURE 2. Block of BK channels by internal Ba^{2+}. (*A* and *B*) Continuous records of current flowing through a single BK channel in an inside-out patch of membrane from cultured rat skeletal muscle in the absence (*A*) and after adding 10 μM Ba^{2+} to the internal solution (*B*). Upward deflections indicate channel opening. (*C*) Blocking and unblocking transitions of the six Ba^{2+} blocks, indicated in *B* with asterisks are presented on a faster time scale. The gaps in the current record during the zero current levels indicate excluded time during the Ba^{2+} blocks. Two of the unblocking transitions occur in two steps, with a transition through a subconductance level (preopening). The solution bathing the normal intracellular side of the membrane (internal solution) contained 500 mM KCl, 100 μM Ca^{2+}, and 5 mM TES buffer. The solution bathing the normal extracellular side of the membrane (external solution) contained 150 mM NMDG-Cl and 5 mM TES buffer. The membrane potential was +30 mV (inside positive).

the normal gating of the channel briefer than the average Ba^{2+} block (Vergarra and Latorre, 1983), which facilitated the identification of the Ba^{2+} blocks. The internal concentration of Ca^{2+} was kept below 250 μM because higher concentrations often induced excessive entry into the low activity mode (Rothberg et al., 1996), and decreased single channel conductance (Oberhauser et al., 1988; Ferguson, 1991).

The novel observation that forms the basis of our study is shown in Fig. 2 *C*, which presents blocking and unblocking transitions on a faster time scale for six of the apparent Ba^{2+} blocks from Fig. 2 *B* (*asterisks*). The transition from the fully blocked to the fully open current level did not always occur in a single step, as might be expected for the exit of a single blocking barium ion, but often proceeded through a subconductance level (preopening) before opening fully, as shown in Fig. 2 *C* (*middle row, left* and *top row, right*). This observation of preopenings was unexpected, since previous studies have shown that the durations of Ba^{2+} blocks are well described by a single exponential, and models typically used to account for Ba^{2+} unblock depict the channel going from fully blocked to fully open in a single step.

In contrast to the preopenings associated with the unblocking of Ba^{2+} in Fig. 2 *C*, the blocking transitions occurred in one step (there were no preclosings), as expected for simple block of the channel by Ba^{2+}.

The brief durations of the preopenings, typically $<\sim$1 ms, may account for why they were not observed in previous studies of Ba^{2+} block, which were optimally performed using low time resolution to capture the slow kinetics of the Ba^{2+} blocking and unblocking rates. It is also possible that preopenings may not be present in BK channels in bilayers.

The preopenings shown in Fig. 2 *C* are different from and should not be confused with the very brief (50–100 μs) lifetime subconductance levels at ~5–10% of the fully open level described by Ferguson et al. (1993) that are associated with both channel opening and closing

in the absence of Ba^{2+}. It will be shown in later sections that the preopenings also differ from the subconductance levels that are entered infrequently during normal gating.

Gating during Preopenings

The form of the two preopenings shown in Fig. 2 *C* was the most common, but other forms were also observed, as shown in Fig. 3, and presents nine additional examples of preopenings from the experiment in Fig. 2. 66% of the preopenings were of the form shown in Fig. 3 *A*, with no closings during the preopening before the full opening from the preopening level; 28% were of the form shown in Fig. 3 *B*, with one or more closings during the preopening before the full opening from the preopening level; and 6% were of the form shown in Fig. 3 *C*, with one or more closings during the preopening before the full opening from the closed level.

It is unlikely that any of the closings observed during the preopenings arose from Ba^{2+} block, because the closings observed during the preopenings typically lasted <1 ms, three orders of magnitude less than the mean duration of the Ba^{2+} blocks. The gating to the zero current level during the preopenings may reflect closing of the gate responsible for normal gating, although activity of the preopening gate cannot be excluded.

Apparent Absence of Preclosings Associated with Ba^{2+} Block

Records from 10 patches were examined for Ba^{2+} blocks. Fig. 4 *C* plots the fraction of examined Ba^{2+} blocks that contained preclosings or preopenings. A typical preopening is shown in Fig. 4 *B*. Fig. 4 *A* presents a drawing of a hypothetical preclosing, since no preclosings were observed in the 10 experiments for Fig. 4. In contrast to the absence of preclosings associated with the 1,202 examined Ba^{2+} blocks, 22.0 ± 3.1% (mean ± SEM) of the Ba^{2+} unblocking transitions contained a preopening.

If microscopic reversibility is obeyed, the number of forward and backward transitions made between any two states should, on average, be equal, and consequently an analysis of the single channel current record either forwards or backwards in time should, on average, yield similar gating sequences (Colquhoun and Hawkes, 1983; Lauger, 1983, 1985; Kirber et al., 1985; Kijima and Kijima, 1987; Steinberg, 1987*a*, 1987*b*). Clearly, the data in Figs. 2 and 4 show that the single channel current records associated with Ba^{2+} block would not yield the same gating, on average, when analyzed either forwards or backwards in time. Preopenings, but no preclosings, would be observed for forward analysis, and preclosings, but no preopenings, would be observed for backwards analysis. Thus, the transitions associated with preopenings violate microscopic reversibility.

The irreversible nature of the preopenings was not due to the osmotic gradient existing in the experiments in Fig. 4. Increasing external NMDG-Cl from 150 to 500 mM to match the 500 mM internal KCl gave the same fraction of Ba^{2+} blocks with preopenings (0.24 ± 0.05, $n = 2$) as with 150 mM external $NMDG^+$ (0.22 ± 0.03, Fig. 4).

The Fraction of Ba^{2+} Blocks Followed by a Preopening Does Not Depend on the Internal Ba^{2+} Concentration

If preopenings require the binding of one or more Ba^{2+} in addition to the blocking Ba^{2+}, then the fraction of preopenings should increase with increasing concentrations of Ba^{2+}. Alternatively, if the single blocking Ba^{2+} is sufficient to induce preopenings, then the fraction of preopenings should be independent of the concentration of Ba^{2+}.

To examine these possibilities, Ba^{2+} was added to the internal solution at concentrations from 0.1 μM to 10 mM. The two traces in Fig. 5 *A* are typical examples of preopenings from data obtained with 1 μM and 1 mM internal Ba^{2+}. Fig. 5 *B* plots the mean of the fraction of

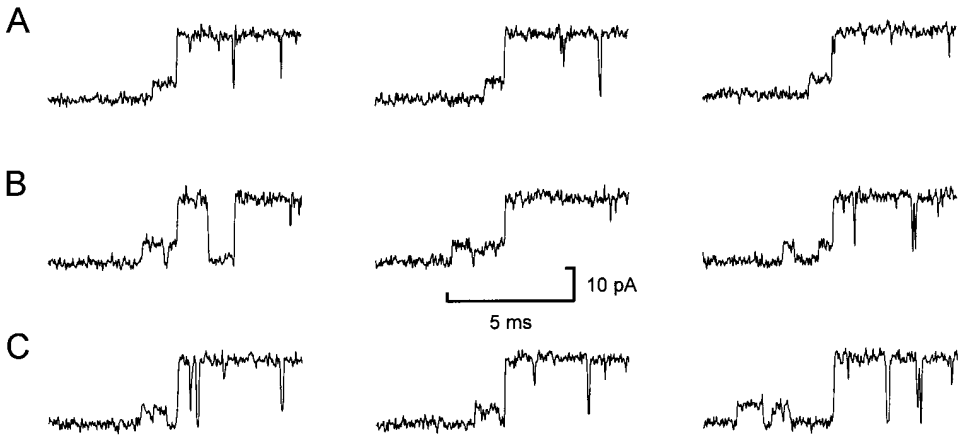

FIGURE 3. Examples of preopenings after Ba^{2+} blocks for three different classes of preopenings (see text). All transitions were from the experiment in Fig. 2 *B*. +30 mV.

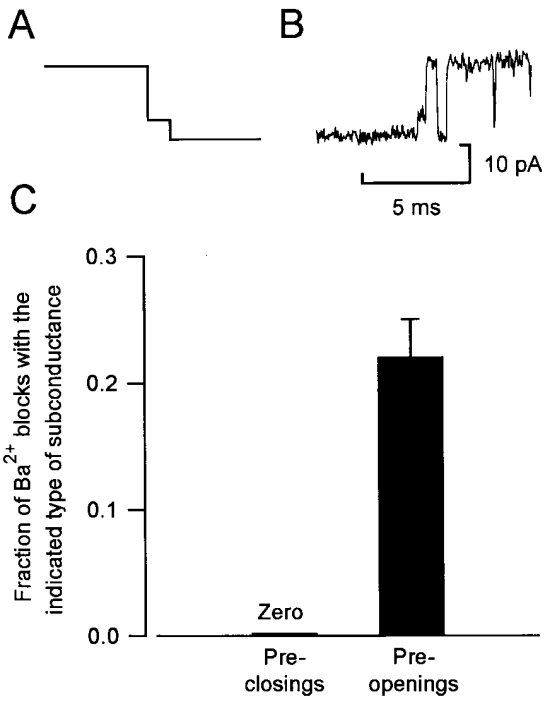

FIGURE 4. Preopenings, but not preclosings, are associated with Ba^{2+} blocks. (*A*) Hypothetical preclosing. (*B*) Typical preopening after a Ba^{2+} block. (*C*) Fraction of Ba^{2+} blocks with preopenings or preclosings. The error bar indicates the SEM for 10 experiments. Same experimental conditions as for Fig. 2. +30 mV.

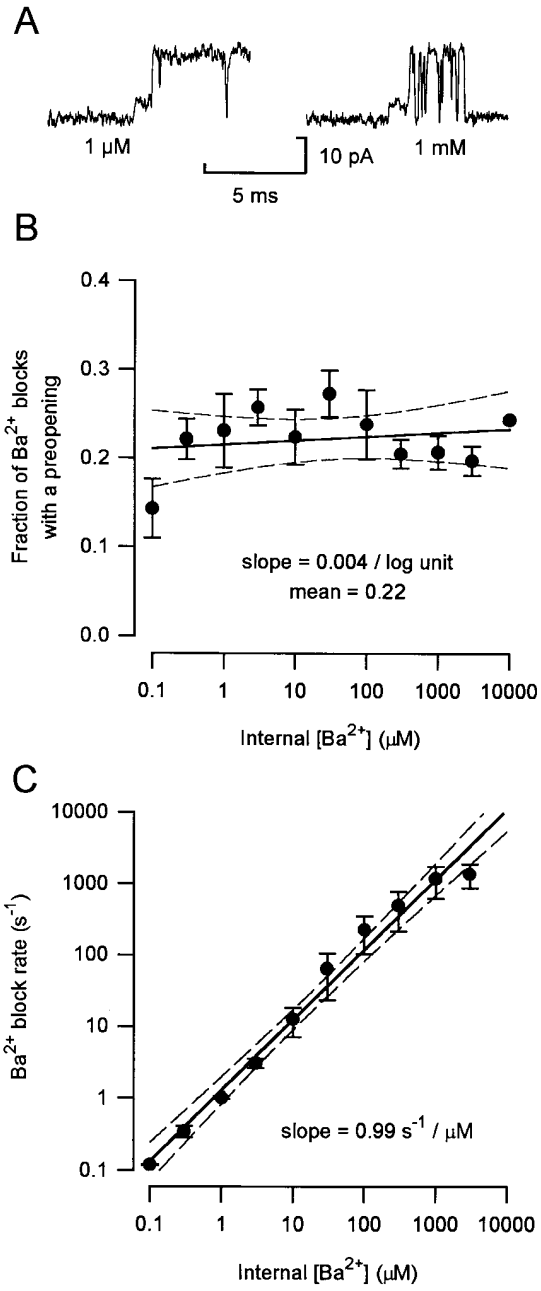

FIGURE 5. Internal Ba^{2+} concentration has little effect on the fraction of Ba^{2+} blocks with a preopening. (*A*) Current traces showing typical preopenings observed in 1 μM and 1 mM internal Ba^{2+}. (*B*) Fraction of Ba^{2+} blocks with a preopening at the indicated concentrations of internal Ba^{2+}. Each plotted symbol with error bars indicates the mean ± SEM of the examined experiments at each concentration. (For *B* and *C* of this figure, and for Figs. 6 and 7, the number of experiments per plotted point were, from left to right: 2, 5, 4, 3, 10, 5, 5, 4, 4, 4, 1.) The continuous line is a least-squares fit to the following equation: fraction = $m\{\log_{10}[[Ba^{2+}]_i(\mu M)]\} + b$, where m is the slope of the line and b is the intercept. In this and the following figures of similar format, the dashed lines represent the 95% confidence limits for the fitted line. Same experimental conditions as for Fig. 2, except for the internal concentrations of Ba^{+}. +30 mV.

Ba^{2+} blocks that contained a preopening at each Ba^{2+} concentration. The continuous line plots a linear regression, and the dashed curves are the 95% confidence limits for the line. The slope of the line was not significantly different from zero ($P > 0.98$). The mean of the plotted points was 0.22. Thus, over a 10^5-fold increase in Ba^{2+} concentration, little or no change was seen in the fraction of Ba^{2+} blocks that terminated in a preopening (Fig. 5 *B*). In contrast, the Ba^{2+} blocking rate increased linearly with Ba^{2+} concentration over the same concentration range (Fig. 5 *C*), consistent with previous observations (Vergara and Latorre, 1983; Neyton and Miller, 1988*a*).

The observation that the number of Ba^{2+} blocks containing a preopening remained a constant fraction of the total number of Ba^{2+} blocks suggests that the single blocking Ba^{2+} ion is sufficient to induce preopenings. (It would, of course, not be possible to detect evidence for two binding sites if one were saturated at Ba^{2+} concentrations >0.1 μM.)

Preclosings were not associated with any of the 6,439 Ba^{2+} blocks analyzed for Fig. 5.

Flickery Block by Millimolar Concentrations of Internal Ba^{2+}

As shown in Fig. 5 *A*, 1 mM internal Ba^{2+} caused an apparent flickery block of the BK channels when the ex-

ternal K^+ was zero. This flickery block was observed for internal Ba^{2+} of 1–10 mM, and is in addition to the long duration Ba^{2+} blocks. The concentrations of Ba^{2+} required for the apparent flickery block are three to four orders of magnitude greater than those required for the long duration blocks, suggesting that the apparent flickery block site has a much lower affinity for Ba^{2+} than the Ba^{2+} block site. Yellen (1984*a*) observed a flickery block of BK channels in chromaffin cells by internal Na^+ when external K^+ was low. Since the internal lock-in site proposed by Neyton and Miller (1988*b*) also binds Na^+ and Ca^{2+}, it is possible that the flickery block by Na^+ (Yellen, 1988*b*) and Ba^{2+} (Fig. 5 *A*) reflects brief binding of these ions to the internal lock-in site. A flickery block of BK channels in epithelial cells by external Ba^{2+} acting at a site near the cytoplasmic side of the pore has been described by Sohma et al. (1996).

The Mean Duration of the Preopenings Does Not Depend on the Internal Ba^{2+} Concentration

Fig. 5 showed that changing the internal Ba^{2+} concentration had little effect on the fraction of Ba^{2+} blocks followed by a preopening. To examine whether changes in internal Ba^{2+} concentration altered the properties of the preopenings that did occur, the duration of each preopening in the records analyzed for Figs. 4 and 5 was measured. Fig. 6 *A* presents examples of preopenings and Fig. 6 *B* plots a cumulative histogram of the durations of preopenings for a single data set (*continuous line*). The distribution was approximated by a single exponential function with a time constant of 0.66 ms (Fig. 6 *B*, *dashed line*). A single exponential decay was observed in the two additional BK channels analyzed in this manner. A single exponential decay is consistent with a single rate constant governing the process terminating the preopenings.

Fig. 6 *C* plots the mean durations of preopenings as a function of internal Ba^{2+} concentration. Over the 10^5-fold change in concentration, there was no significant effect of Ba^{2+} on the mean duration of the preopenings ($P > 0.7$), indicating that the rate constant for the transition from the preopening level to the fully conducting open level was independent of Ba^{2+} concentration. The mean duration of the preopenings was 0.69 ms.

The Fractional Conductance of Preopenings Does Not Depend on the Internal Ba^{2+} Concentration

Fig. 7 plots the fractional current amplitude of the preopenings as a function of the concentration of internal Ba^{2+}. The fractional current amplitude for each observed preopening was determined by dividing the current amplitude during the preopening by the fully open current amplitude after the preopening. An average fractional amplitude was then determined for the

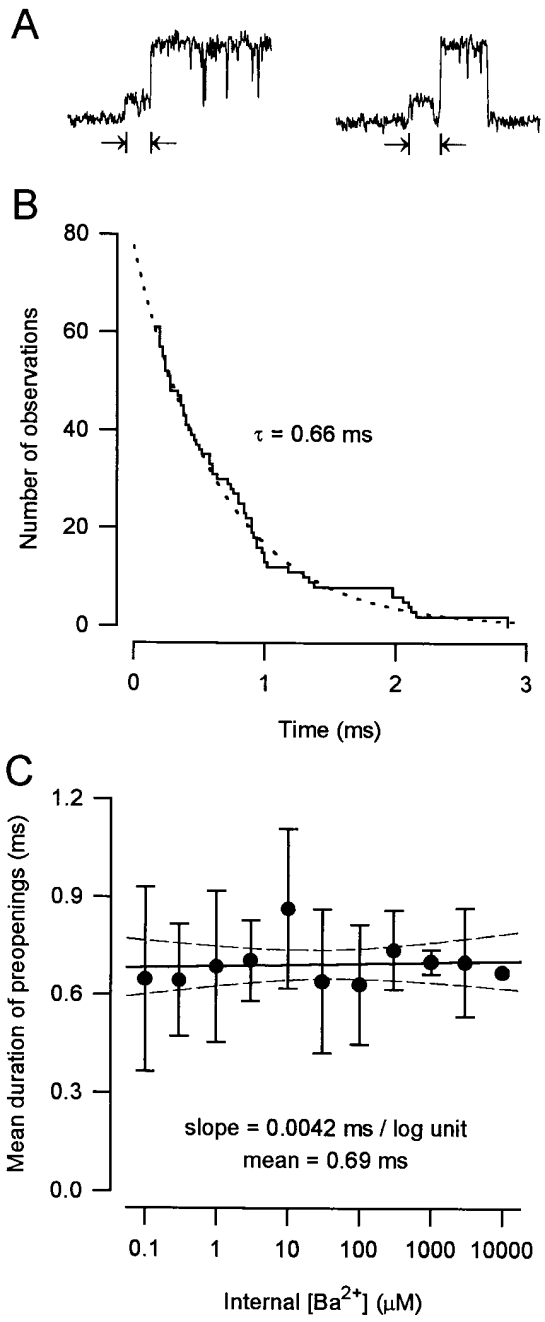

FIGURE 6. Internal Ba^{2+} concentration has little effect on the mean duration of the preopenings. (*A*) Current traces showing that the duration of the preopenings was measured from the start of the preopening to the time of the transition to the fully open level, including any closed time during this period. (*B*) Cumulative distribution of the durations of the preopenings are measured as shown in *A*. The continuous line plots the number of preopenings lasting as long or longer than the indicated duration. The dashed line is the maximum likelihood fit to a single exponential function of the following form: No. of observations = $A \exp(-t/\tau)$, where A is the total number of preopenings in the distribution, τ is the time constant (mean duration) of the intervals in the distribution, and exp is an exponential function. 10 μM internal Ba^{2+}. (*C*) Mean duration of the preopenings at the indicated internal Ba^{2+} concentrations. Same experimental conditions and experiments as for Fig. 5. +30 mV.

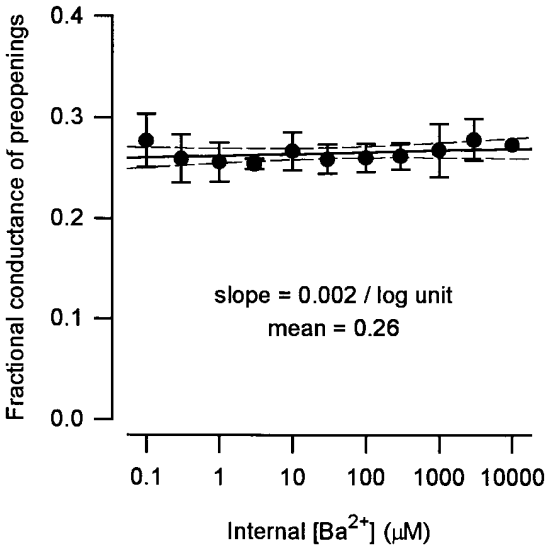

FIGURE 7. Internal Ba^{2+} concentration has little effect on the fractional conductance of preopenings. The fractional amplitudes of the preopenings are plotted against the Ba^{2+} concentrations. Same experimental conditions and experiments as in Fig. 5. +30 mV.

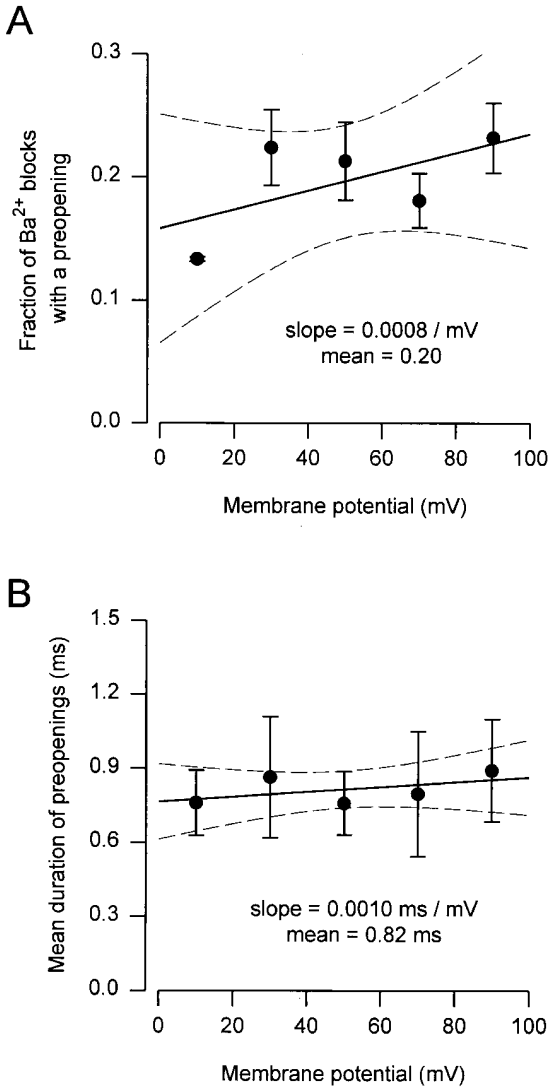

FIGURE 8. Effect of membrane potential on the fraction of Ba^{2+} blocks with a preopening (*A*) and on the mean duration of the preopenings (*B*). Each plotted symbol with error bars indicates the mean ± SEM of the examined experiments at the indicated voltage. For *A* and *B* of this figure, and for Fig. 9, *B* and *C*, the numbers of experiments per plotted point were (from left to right): 2, 10, 5, 3, 2. Same experimental conditions as for Fig. 2.

preopenings in each data set. Ba^{2+} had an insignificant effect on the fractional conductance of the preopening ($P > 0.28$). The mean of all the experiments indicated that the typical preopening was a transition to a subconductance level at 26% of the full conductance level.

The results in Figs. 2–7 show that changes in Ba^{2+} concentration over five orders of magnitude have insignificant effects on the duration and conductance of the preopenings, or on the fraction of Ba^{2+} blocks followed by a preopening. Apparently, the single Ba^{2+} ion that blocks the channel suffices to induce the preopening.

Voltage Dependence of the Fraction of Ba^{2+} Blocks Containing a Preopening

If the Ba^{2+}-induced alteration in the channel responsible for the preopenings involves rate-limiting voltage-dependent movement of charge through the electric field of the membrane, then changes in membrane potential may alter the kinetic and/or conductance properties of the preopenings. To test this possibility, currents were recorded at membrane potentials ranging from +10 to +90 mV with 0 K^+ outside (same as for Figs. 2–7). Under these conditions, the dissociation of the blocking Ba^{2+} ion would be to the external solution (see INTRODUCTION and Neyton and Miller, 1988*a*, 1988*b*).

Fig. 8 *A* plots the fraction of Ba^{2+} blocks followed by a preopening as a function of membrane potential. There was a tendency for the fraction of Ba^{2+} blocks associated with preopenings to increase with depolarization (slope of 0.0008/mV), but the increase was not statistically different from zero ($P > 0.28$). The mean fraction of Ba^{2+} blocks associated with preopenings was 0.20 for the data in the figure. (Examples of current traces at different voltages will be presented in a later figure.)

Over the same range of voltages, the mean durations of the Ba^{2+} blocks decreased from 5.9 s at +10 mV to 1.2 s at +90 mV (not plotted), consistent with the membrane potential driving Ba^{2+} through the channel to the external solution.

Over the range of membrane potentials tested, none of the 2,176 Ba^{2+} blocks analyzed for Fig. 8 *A* contained a preclosing.

The Mean Duration of the Preopenings Is Independent of Membrane Potential

The durations of the preopenings for the data sets examined for Fig. 8 *A* were measured and plotted in Fig. 8 *B*. Voltage had an insignificant effect on the durations ($P > 0.37$), which had a mean value of 0.82 ms. The observation that the durations of the preopenings were little affected by membrane potential suggests that the process by which preopenings make transitions to full openings is not rate limited by a voltage-dependent step.

The Fractional Amplitude of Preopenings Increases with Depolarization

Fig. 9 *A* presents current traces of preopenings recorded at different membrane potentials from one of the experiments included in Fig. 8. The ratio of the amplitude of the preopenings to that of the full openings increased with increasing membrane potential. This is shown more clearly in Fig. 9, which plots the current amplitudes of both the preopenings and the full openings versus membrane potential (Fig. 9 *B*), and the ratios of the current amplitudes of the preopenings to the current amplitudes of the full openings (Fig. 9 *C*).

The preopening amplitude increased from 24 to 39% of the fully open amplitude as the membrane potential was increased from +10 to +90 mV. The fractional increase in amplitude was 0.002/mV (continuous line in Fig. 9 *C*). The observations in Fig. 9 suggest that membrane potential has a differential effect on the conductance during the preopening and fully open levels.

Preopenings Arise from a Different Mechanism than Subconductance Levels during Normal Gating

BK channels occasionally enter subconductance levels during normal gating in the absence of Ba^{2+} (Barrett et al., 1982; Moczydlowski and Latorre, 1983; Stockbridge and French, 1989; Stockbridge et al., 1991; Miller et al., 1987) have shown that the gate in BK channels can open and close when the channels are blocked by Ba^{2+}. Thus, the possibility arises that the preopenings associated with Ba^{2+} block are not induced by the blocking Ba^{2+} ion, but simply reflect chance gating to a subconductance level at the time Ba^{2+} unblocks. If this is the case, then the conductance level of the preopenings and subconductance level should be the same, and the conductance during the subconductance levels should have the same voltage dependence as was observed for the preopenings in Fig. 9. To examine this possibility, the fractional conductance and voltage dependence of the subconductance levels during normal gating were determined and compared with values obtained for the preopenings.

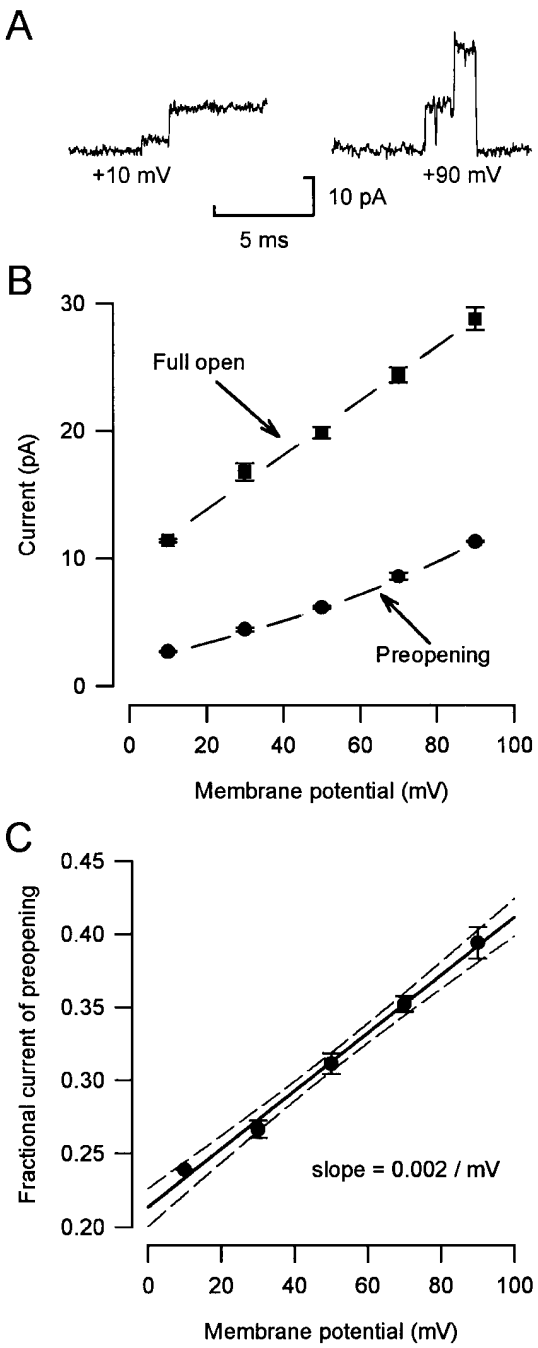

FIGURE 9. The fractional conductance of preopenings increases when the membrane potential is made more positive. (*A*) Current traces of typical preopenings observed at +10 and +90 mV. (*B*) Current–voltage plot for the preopening and fully open current levels. The dashed lines have no theoretical basis. (*C*) Fractional current of the preopenings compared with the fully open current at the indicated membrane potentials. The slope of the fitted line was significantly different from zero ($P < 0.0001$). Same experimental conditions and experiments as for Fig. 8.

Results from two channels (plotted as black and gray bars) are shown in Fig. 10. Current records at +90 mV during a transition to a subconductance level during normal activity and during a preopening are shown in

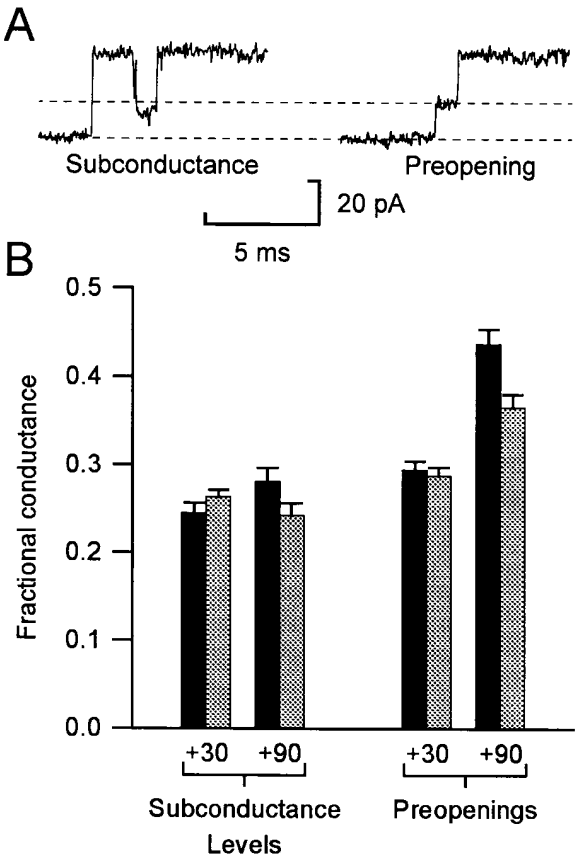

FIGURE 10. Preopenings are different from subconductance levels observed during normal gating. (*A*) Current traces recorded at +90 mV of a typical subconductance level observed during normal gating and of a typical preopening. (*B*) Mean fractional conductances of all subconductance levels <50% of the fully open level during normal gating and of preopenings. Estimates were made at both +30 and +90 mV. The black and gray bars plot the results for two separate channels. The subconductance levels were obtained from currents recorded in the absence of added Ba^{2+} and the preopenings were recorded with 10 μM internal Ba^{2+}. The concentrations of the other ions in the solutions were the same as for Fig. 2.

Fig. 10 *A*. As typically observed in comparisons of this type, the conductance of the preopening was greater than that of the subconductance levels. Fig. 10 *B* plots the average fractional conductances. At +90 mV, the average fractional conductance was 53% greater for the preopenings than for the subconductance levels ($P < 0.005$). The greater conductance of the preopenings at +90 mV was mainly due to the fact that the fractional conductance of the preopenings was voltage dependent (as shown previously in Fig. 9), increasing an average of 38% for these two experiments when voltage was changed from +30 to +90 mV ($P < 0.05$). In contrast, the average fractional conductance of the subconductance levels was insignificantly affected by voltage, increasing slightly in one experiment and decreasing in the other ($P > 0.7$).

For the experiments presented in Fig. 10, the subconductance levels during normal gating were measured in the absence of internal Ba^{2+} to remove the possibility that any of those measured may have been associated with a brief Ba^{2+} block, as subconductance levels can also occur immediately after complete closings. Measurements of subconductance levels during normal gating were also made from the same membrane patch in the presence of Ba^{2+} and were found to be essentially the same as the subconductance levels in Fig. 10 (not shown). Thus, the fractional amplitude of the subconductance levels lacked voltage dependence both in the presence and absence of Ba^{2+}.

The greater conductance and voltage dependence of the fractional conductance for preopenings when compared with subconductance levels indicates that the mechanisms underlying preopenings and subconductance levels are different. Thus, since the preopenings are not normal subconductance levels, then Ba^{2+} must induce the preopenings.

Additional support that preopenings do not reflect gating to normal subconductance levels at the time that Ba^{2+} unblocks comes from the low fraction of time that BK channels spend in subconductance levels during normal gating. Analysis of single channel current records in the absence of Ba^{2+} for the two channels analyzed for Fig. 10 indicated that the average fraction of time spent in subconductance levels during normal gating was ~0.0012. This is similar to the low value of ~0.001 observed previously (Barrett et al., 1982), and can be compared with the fraction of Ba^{2+} blocks ending with a preopening of typically 0.22 in experiments of this type (Fig. 5). Thus, the fraction of Ba^{2+} blocks with preopenings was more than two orders of magnitude greater than what would have been expected by chance alone if preopenings simply reflected the random unblocking of channels by Ba^{2+} at the time the channels were gating to subconductance levels, suggesting once again that Ba^{2+} induces the preopenings.

External K^+ Reduces the Fraction of Ba^{2+} Blocks with Preopenings

Neyton and Miller (1988*b*) found that whether the blocking Ba^{2+} dissociates to the external or internal solution depends on the concentration of K^+ in the external solution. With 0 K^+ and 150 mM $NMDG^+$ in the external solution, Ba^{2+} preferentially dissociates to the external solution, as indicated by the shortening of the blocked intervals by depolarization. With >10 mM K^+ in the external solution, Ba^{2+} binds to the external lock-in and enhancement sites, forcing Ba^+ to preferentially dissociate to the internal solution, as indicated by a reversed voltage dependence of the duration of the blocked intervals.

To examine if the fraction of Ba^{2+} blocks with pre-

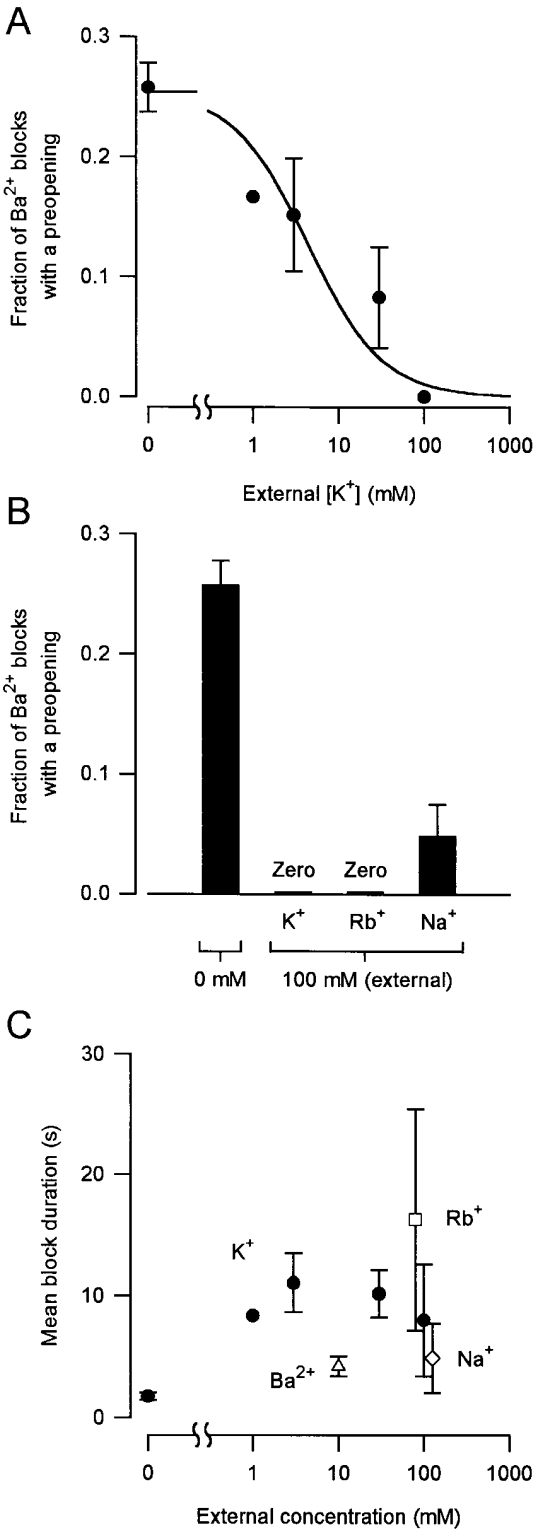

FIGURE 11. External K^+, Rb^+, or Na^+ reduces the fraction of blocks with preopenings. (*A*) Fraction of Ba^{2+} blocks that contain a preopening in the presence of the indicated external K^+ concentrations with equimolar replacement of external $NMDG^+$ with K^+. The internal Ba^{2+} was 3 μM. The cation in the internal solution was 500 mM K^+. Each of the plotted symbols with error bars indicate the mean ± SEM for the experiments under the indicated conditions. The numbers of experiments per plotted point were (from left to right): 3, 1, 3, 2, 5. The continuous line is a least-squares fit by the inhibition equation: fraction = $f_{max} - \{f_{max}/[1 + ([K^+]_o/K_i)]\}$, where f_{max} is the fraction of Ba^{2+} blocks that contain a preopening with 0 mM external K^+, and K_i is concentration at half maximal inhibition. The fitted K_i is 6.6 mM and the fitted f_{max} is 0.26. (*B*) Fraction of Ba^{2+} blocks with a preopening with 100 mM external Rb^+ or Na^+ replacing 100 mM $NMDG^+$. The bars for 0 and 100 mM external K^+ are replotted from *A* for comparison. Each bar with associated error bar indicates the mean ± SEM for (left to right) 3, 5, 3, and 4 data sets. (*C*) Mean duration of the Ba^{2+} blocks observed at the indicated external ion concentration for the experiments shown in *A* and *B*. Each symbol (● for K^+, □ for Rb^+, ◇ for Na^+, and △ for Ba^{2+}) plots the average of the time constants obtained from the fits to the exponential component defining Ba^{2+} block (see METHODS). The experiments are the same as in *A* and *B*, except for Ba^{2+}, which is from four experiments.

openings changed with the concentration of external K^+, and consequently the direction of Ba^+ dissociation, currents were recorded with increasing amounts of K^+ replacing equal molar amounts of the $NMDG^+$ in the extracellular solution. Fig. 11 *A* plots the fraction of Ba^{2+} blocks with a preopening versus external K^+ concentration. As external K^+ was increased, the fraction of Ba^{2+} blocks with preopenings decreased until, at 100 mM external K^+, preopenings were no longer observed. The continuous curve in Fig. 11 *A* is a nonlinear least-squares fit of the plotted points to a rectangular hyperbola with a K_i for inhibition of preopenings by K^+ of 6.6 mM (details in figure legend).

The observation that the fraction of preopenings was decreased as external K^+ was increased is consistent with the notion that preopenings can occur only when Ba^{2+} dissociates to the external solution. (The possibility that external K^+ prevents preopenings through direct allosteric modification of the channel, rather than by preventing Ba^{2+} from dissociating to the external solution, cannot be excluded.)

External Rb^+ and Na^+ also Reduce the Fraction of Ba^{2+} Blocks with Preopenings

If the decrease in the fraction of preopenings with increasing external K^+ shown in Fig. 11 *A* were due to the binding of K^+ to the external lock-in site so that Ba^{2+} had to dissociate to the intracellular solution, then other ions that bind to these sites should also decrease the fraction of preopenings. Neyton and Miller (1988*a*) found that external Rb^+ was more effective than external K^+ in binding to the external lock-in site, and that external Na^+ could also bind, but much less effectively.

To examine whether permeant Rb^+ and impermeant Na^+ (Blatz and Magleby, 1984) also reduced the fraction of preopenings, 100 mM Rb^+ or Na^+ was added

to the extracellular solution, replacing equal molar amounts of $NMDG^+$. The results are shown in Fig. 11 *B*, which plots the fraction of Ba^{2+} blocks containing a preopening for each of the indicated conditions. The data with 0 and 100 mM external K^+ are from Fig. 11 *A* for comparison. As was the case for 100 mM external K^+, addition of 100 mM Rb^+ to the external solution also eliminated the preopenings. External Na^+ at 100 mM, while not eliminating the preopenings, did reduce the fraction of Ba^{2+} blocks with preopenings to 0.05 ± 0.03 compared with 0.25 ± 0.02 with external $NMDG^+$ and no external Na^+. Thus, external K^+ and Rb^+, two ions that are more effective than external Na^+ in binding to the external lock-in site (Neyton and Miller, 1988*a*), were also more effective than Na^+ in eliminating preopenings.

Preopenings Can Be Observed with External Ba^{2+}

For the experiments presented in the previous sections, the blocking Ba^{2+} ion entered the pore of the channel from the internal side, since Ba^{2+} was added to the internal solution. Ba^{2+} can also enter and block BK channels from the external solution, but much higher concentrations of Ba^{2+} are required to achieve the same blocking rate as compared with block from the internal solution (Vergarra and Latorre, 1983; Miller et al., 1987; Neyton and Miller, 1988*a*). Independent of whether Ba^{2+} enters from the external or internal solution, Ba^{2+} appears to block at the same site in the conduction pathway, with the barriers to reaching the blocking site being greater from the external solution (Vergarra and Latorre, 1983; Neyton and Miller, 1988*a*, 1988*b*).

To test whether Ba^{2+} could also induce preopenings when entering the channel from the external solution, currents were recorded with 10 mM Ba^{2+} added to either the external or internal solutions. Of 428 identified Ba^{2+} blocks in four separate experiments in 10 mM external Ba^{2+}, 8 were associated with preopenings. These results are summarized in Fig. 12 *B*, which shows that the fraction of Ba^{2+} blocks with preopenings with 10 mM external Ba^{2+} was only 0.019, 13-fold less than the fraction of 0.24 observed with 10 mM internal Ba^{2+}.

The vast majority of the Ba^{2+} blocks observed with 10 mM external Ba^{2+} would have arisen from Ba^{2+} entering and blocking the channel from the external solution, and not from any contaminant Ba^{2+} entering and blocking the channel from the internal solution, as the Ba^{2+} block rate of 2.0 s^{-1} for 10 mM external Ba^{2+} was 60-fold greater than the contaminant Ba^{2+} blocking rate of 0.032 s^{-1} (mean from nine experiments) when Ba^{2+} was not added to either solution.

Although 98.4% ($1 - [0.032\ s^{-1}/2\ s^{-1}]$) of the blocks would have arisen from external Ba^{2+}, the possibility exists that the preopenings were generated only from the remaining 1.6% of the blocks arising from contaminating internal Ba^{2+}. If preopenings arose only from blocks from internal Ba^{2+}, then, assuming that 22% of such blocks had preopenings, the fraction of Ba^{2+} blocks with preopenings should have been 0.0035 (0.22×0.016), a value approximately fivefold less than the observed value of 0.019 in 10 mM external Ba^{2+}. Thus, these calculations would suggest that external Ba^{2+} can both block the channel and generate some preopenings, although less than for internal Ba^{2+}.

If the Ba^{2+} blocking site is the same for internal or external Ba^{2+}, then it might be expected that the fraction of preopenings would be independent of the side from which Ba^{2+} entered the channel, in contrast to the findings in Fig. 12 *B*. A possible explanation for this apparent paradox is offered by the observations of Neyton and Pelleschi (1991), who found that external Ba^{2+} can act like external K^+ by binding to the external lock-in site, preventing the exit of Ba^{2+} to the external solution. On this basis, since external K^+, which forces the exit of the blocking Ba^{2+} to the internal solution, reduces the fraction of Ba^{2+} blocks with preopenings

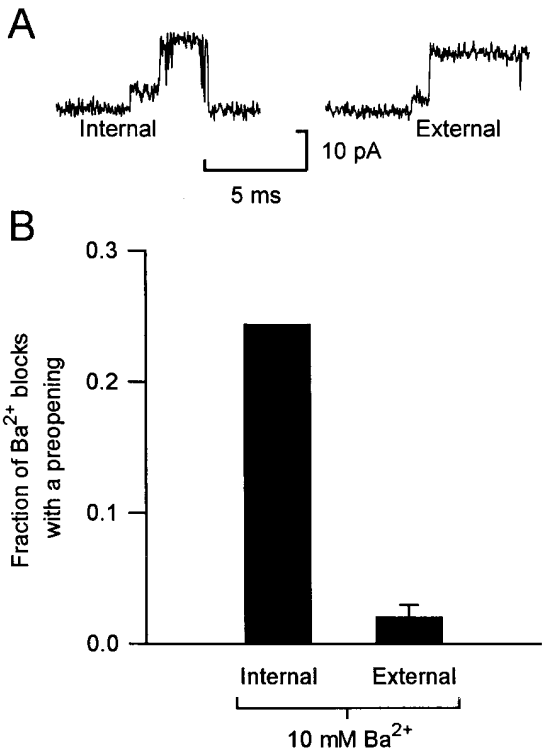

FIGURE 12. Preopenings are observed with Ba^{2+} in the external solution. (*A*) Current traces of preopenings observed in the presence of 10 mM internal or external Ba^{2+}. (*B*) Fraction of Ba^{2+} blocks with a preopening in the presence of 10 mM internal or external Ba^{2+}. The bar for 10 mM internal Ba^{2+} is replotted from the data in Fig. 5. The mean ± SEM with 10 mM external Ba^{2+} is based on data from four experiments.

(Fig. 11), external Ba^{2+}, which also forces the exit of the blocking Ba^{2+} to the inside, might also be expected to reduce the fraction of Ba^{2+} blocks with preopenings, as was observed (Fig. 12). Evidence for two Ba^{2+} binding sites in the pore of K^+ channels has also been obtained by Hurst et al. (1995) and Sohma et al. (1996).

Preopenings Are Not Observed when the Blocking Ba^{2+} Ion Dissociates to the Internal Solution

A common observation in Figs. 11 and 12 is that experimental conditions that would have been expected to block the exit of Ba^{2+} to the external solution (100 mM external K^+ or 100 mM external Rb^+) completely eliminated the preopenings, and solutions that would be expected to reduce but not eliminate the exit of Ba^{2+} to the external solution (1–30 mM external K^+, 10 mM external Ba^{2+}, or 100 mM external Na^+) reduced but did not eliminate preopenings. Thus, these observations suggest that preopenings are associated with the dissociation of Ba^{2+} to the external solution.

Relationship between Mean Duration of Ba^{2+} Blocks and the External Lock-In Ions

Fig. 11*C* plots the mean duration of Ba^{2+} blocks as a function of the concentrations of the various external ions examined. These results are consistent with the observations of Neyton and Miller (1988*a*, 1988*b*), who found that Ba^{2+} block duration increased as external K^+ was increased from 0 to 10 mM (due to binding to the external lock-in site to prevent dissociation to the external solution), and then decreased as external K^+ was increased to several hundred millimolar (due to binding to the external enhancement site, forcing dissociation of Ba^{2+} to the internal solution). Neyton and Miller (1988*a*, 1988*b*) also found that Ba^{2+} blocks were longer in 100 mM external Rb^+ and shorter in 100 mM external Na^+ than they were in 100 mM external K^+. The lack of strong correlation in the data in Figs. 11 and 12 between the duration of Ba^{2+} blocks and the fractions of Ba^{2+} blocks with preopenings reflects the observation that the fraction of preopenings depends on the direction of exit of Ba^{2+} from the channel (see above section), which is not necessarily tightly coupled to the duration of the Ba^{2+} blocks.

Only One Apparent Preclosing in ~10,000 Examined Ba^{2+} Blocks

Only one apparent preclosing was observed during this entire study of ~10,000 Ba^{2+} blocks examined for preopenings and preclosings. This one apparent preclosing was in one of the data sets with 3 mM external K^+ analyzed for Fig. 11 *A*. As mentioned in a previous section, BK channels spend ~0.1% of their open time during normal gating in subconductance levels. Thus, it is possible that this apparent preclosing represented a transition to a subconductance level during normal gating that occurred by chance just before a Ba^{2+} block. If this is the case, then the irreversible mechanism generating the preopenings may be strictly unidirectional.

DISCUSSION

The Opening Transition Associated with Ba^{2+} Unblock is More Complex than Previously Thought

Ba^{2+} blockade of BK channels from rat skeletal muscle has been well characterized at the single-channel level (Vergarra and Latorre, 1983; Miller, 1987; Miller et al., 1987; Neyton and Miller, 1988*a*, 1988*b*; Neyton and Pelleschi, 1991). Ba^{2+} enters the open channel and blocks the flow of ions. After a mean block time of several seconds, Ba^{2+} dissociates and leaves the channel, thus immediately restoring the current to the full open level seen before the block.

Our results were consistent with this picture when high concentrations of K^+ were present in the external solution. However, when the external K^+ concentration was ≤30 mM, our observations indicated that the unblocking of the channel could be associated with the transition of the channel through a subconductance level (Figs. 2–7). This subconductance level, with a mean duration of 0.75 ms and a conductance of ~26% of the fully open level (+30 mV) was termed a preopening since it preceded the current transition to the fully open level from the blocked level. Preopenings were present in 0.22 of the unblocking transitions with 150 mM external $NMDG^+$, and this fraction was independent of the concentration of the internal Ba^{2+} used to block the channel.

Only one possible preclosing, defined as a subconductance level immediately preceding a Ba^{2+} block, was observed in the ~10,000 examined Ba^{2+} blocking transitions. It was likely that this one exception was a chance transition through one of the subconductance levels that occurred infrequently during normal activity. Thus, the preopenings appear to represent absolute time-irreversible subconductance gating. In contrast to the preopenings after Ba^{2+} block, normal gating appears consistent with microscopic reversibility (McManus and Magleby, 1989; Song and Magleby, 1994).

Preopenings Are Not Observed when the Blocking Ba^{2+} Ion Is Forced to Dissociate to the Internal Solution

Addition of K^+ to the external solution by equimolar replacement of the $NMDG^+$ reduced the fraction of Ba^{2+} blocks followed by preopenings (Fig. 11). With 100 mM external K^+ or Rb^+, preopenings were no longer observed even though Ba^{2+} blocks were still present. External Na^+ and Ba^{2+} also reduced the fraction of Ba^{2+} blocks (Figs. 11 and 12). Neyton and Miller (1988*b*)

have previously shown a reversal in the sign of δ, the fraction of the membrane electric field sensed by Ba^{2+}, as external K^+ was increased. They concluded that the side of the membrane to which Ba^{2+} dissociated from the channel changed from outward to inward as external K^+ was increased. External Na^+, Rb^+, and Ba^{2+} could also shift the direction of dissociation from the external side to the internal side (Neyton and Miller, 1988*b*; Neyton and Pelleschi, 1991).

Thus, under conditions where Ba^{2+} would be expected to dissociate to the external solution, preopenings were observed following Ba^{2+} blocks. However, under conditions where Ba^{2+} would have been expected to dissociate preferentially to the internal solution, preopenings were seen less frequently or not at all. The following section examines two functionally different models consistent with these observations. In the first model, Ba^{2+} itself forms the subconductance gate.

Model 1 for Irreversible Subconductance Gating: Bound Ba^{2+} Forms the Preopening Gate

In the first model to be considered, the preopenings arise directly from Ba^{2+} binding to a preopening site in the channel that is located external to the Ba^{2+} block site. When Ba^{2+} binds to this site, which is normally occupied by K^+, the conductance is reduced, creating a preopening. Fig. 13 *A* depicts the gating with 0 mM external K^+. The only ions depicted are K^+ at the preopening site and Ba^{2+}. The four K^+ ions that Neyton and Miller (1988*b*) suggest are typically in the conducting channel in the absence of Ba^{2+} block are not shown. The preopening site may bind one of the four K^+, but this is not known. The open unblocked channel (state 1) becomes blocked after Ba^{2+} enters the channel from the internal solution (state 2). Once in state 2, there are two possible outcomes. Unblocking can occur without a preopening if Ba^{2+} dissociates directly to either the internal or external solution (state 1). Alternatively, if the K^+ bound to the preopening site in state 2 dissociates to the external solution before Ba^{2+} unblocks, then the channel makes an irreversible transition to state 3. The preopening site remains unoccupied by K^+ because the outside solution contains no K^+, and the blocking Ba^{2+} ion prevents internal K^+ from reaching the preopening site.

Ba^{2+} can then move from the blocking site (state 3) to the unoccupied preopening site (state 4) to generate a preopening through partial obstruction of the channel. After ~0.75 ms, Ba^{2+} then dissociates to the outside, and one of the K^+ ions moving down the channel immediately occupies the preopening site, restoring the conductance to the fully open current level (state 1).

The transition from state 2 to 3 for the dissociation of

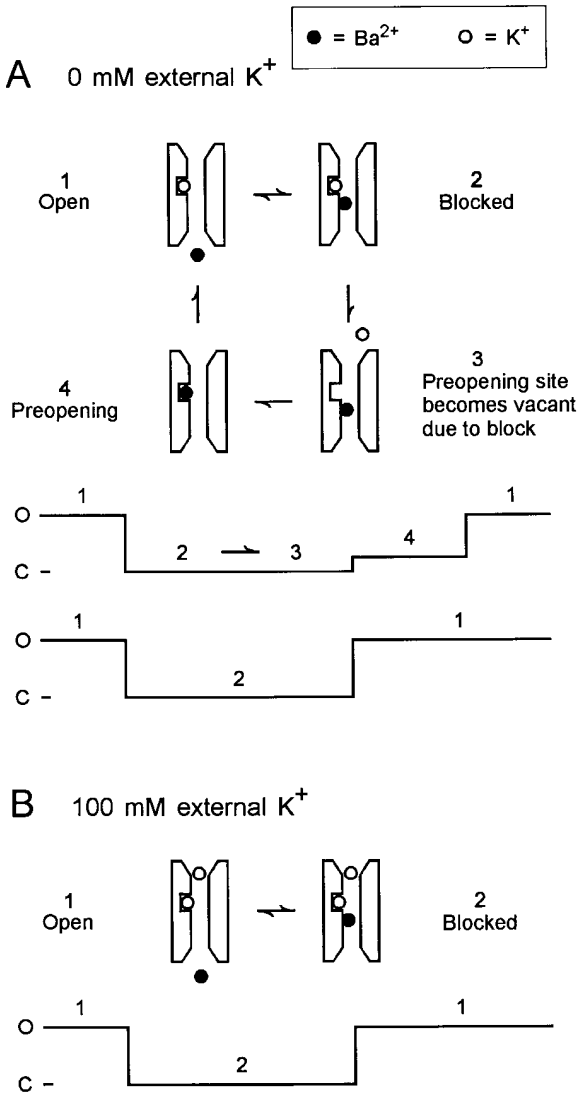

FIGURE 13. Model 1. A cartoon for generation of preopenings when Ba^{2+} forms the preopening gate. (*A*) Generation of preopenings with 0 mM external K^+. Below the model are hypothetical single-channel currents and indicated state transitions for Ba^{2+} blocks with (*top*) and without (*bottom*) preopenings. (*B*) Absence of preopenings with 100 mM external K^+. See text for descriptions of the models.

K^+ to the external solution is irreversible since the single K^+ ion is lost into the external solution, which contains 0 K^+. The transition from state 3 to 4 is also apparently irreversible, since the positive membrane potential and the outward flux of K^+ would drive Ba^{2+} away from the blocking site, and the entering K^+ would immediately occupy the site once Ba^{2+} left. Support for the effective irreversibility of step 3 to 4 comes from the observation that preopenings were not observed between two Ba^{2+} blocks, as would occur for the hypothetical transition sequence among states 1–2–3–4–3–4–1.

The transition from state 4 to 1 has been drawn as ir-

reversible, as the entering K^+ would immediately occupy the preopening site as soon as Ba^{2+} leaves, returning the channel to the initial state 1. We cannot rule out, however, that the step might be reversible. Our lack of observations of preclosings would not require that the step be irreversible since a preclosing is defined as a transition from the open level to a subconductance level followed by a Ba^{2+} block. The irreversibility of the transition from state 3 to 4 would be sufficient to prevent preclosings even if the transition from state 4 to 1 were reversible.

Below the model (Fig. 13 *A*) are hypothetical current records with state transitions for Ba^{2+} block with (*top*) and without (*bottom*) a preopening. The channel typically makes approximately three blocking transitions without for every one with a preopening. The gating that can occur during the preopenings (see examples in Figs. 3, 6, and 9) is not incorporated into the model in Fig. 13 and may reflect gating of the main gate during the preopening.

External K^+, Rb^+, Na^+, and Ba^{2+} can bind to sites external to the Ba^{2+} blocking site, preventing the dissociation of the blocking Ba^{2+} to the external solution (Neyton and Miller, 1988*a*; Neyton and Pelleschi, 1991) and preventing preopenings (Figs. 11 and 12). Thus, it is not unreasonable to assume that these ions might prevent the blocking Ba^{2+} from binding to the preopening site.

On this basis, Fig. 13 *B* depicts the gating with 100 mM external K^+ (or Rb^+) where no preopenings are seen (Fig. 11). The open unblocked channel (state 1) becomes blocked after Ba^{2+} enters the channel from the internal solution (state 2). However, the high concentrations of K^+ (or Rb^+) in the external solution prevents the movement of Ba^{2+} to the preopening site. Hence, no preopenings are seen, as shown in the hypothetical current record with state transitions below the model. The graded decrease in the fraction of preopenings with increasing external K^+ (Fig. 11 *A*) would reflect a progressive shift from the gating shown in Fig. 13 *A* to that shown in Fig. 13 *B,* as the increasing external K^+ (or Rb^+) prevented Ba^{2+} from binding to the preopening site, either by titrating the site or by repulsion.

The relationship of the preopening site in the model in Fig. 13 to the external lock-in and enhancement sites described by Neyton and Miller (1988*a*, 1988*b*) is not clear. The K_i of 6.6 mM for the inhibition of preopenings by external K^+ in our experiments (Fig. 11 *A*) differed by two orders of magnitude from both the K_i of 20 μM for the external lock-in site and $K_d > 500$ mM for the external enhancement site in the experiments of Neyton and Miller (1988*a*, 1988*b*), suggesting that there may not be a direct one-to-one relationship between the preopening site and either the external lock-in or enhancement sites.

For the model in Fig. 13, the reduced conductance of the preopenings arises from the constricted flow of K^+ past a Ba^{2+} bound to the preopening site. If the preopening site is within the pore of the channel, then this model would require that at least one part of the channel be wider than suggested by the strictly single file model of Neyton and Miller (1988*b*).

Up to this point, Model 1 in Fig. 13 has been discussed from the viewpoint of the blocking Ba^{2+} coming from the internal solution. Preopenings were also seen with external Ba^{2+}, where the fraction of Ba^{2+} blocks with preopenings was approximately fivefold less than for internal Ba^{2+} (Fig. 12). In terms of model 1, the external Ba^{2+} would have to pass the preopening site to reach the Ba^{2+} blocking site. This may account in part for why block by external Ba^{2+} requires an ~1,000-fold higher concentration of Ba^{2+} for the same blocking rate. Once Ba^{2+} reaches the Ba^{2+} blocking site, which is at the same location for block by external or internal Ba^{2+} (see INTRODUCTION), the sequence of events for irreversible subconductance gating would be the same as described above for internal Ba^{2+}. Since the millimolar concentrations of external Ba^{2+} required to block the channel from the external side also act like external K^+ (Neyton and Pelleschi, 1991), in preventing the exit of Ba^{2+} to the external solution, as in Fig. 13 *B,* then this could account for why fewer preopenings are seen with external Ba^{2+}.

Model 2 for Irreversible Subconductance Gating: Ba^{2+} Induces the Preopening Gate

In the second model to be considered for the preopenings, Ba^{2+} acts allosterically to induce a preopening gate that constricts the channel (either electrostatically or sterically) as shown in Fig. 14. In this model, the Ba^{2+}-induced preopening gate both reduces the conductance of the channel and also prevents the exit of Ba^{2+} to the internal solution. A Ba^{2+}-induced preopening gate that prevents exit of Ba^{2+} to the internal solution is similar to the carrier-like behavior of an ion channel that can be generated with shifting energy barriers, as described by Lauger (1983, 1985).

While we have no direct evidence that Ba^{2+} can induce the required conformational change, previous experiments on K^+ channels have suggested that the blocking Ba^{2+} can influence the conformation of the channel by stabilizing either the open or closed state, depending on the experimental conditions (Armstrong and Taylor, 1980; Miller et al., 1987; Neyton and Miller, 1988*a*; Neyton and Pelleschi, 1991).

Fig. 14 *A* depicts the gating with 0 mM external K^+. The open unblocked channel (state 1) becomes blocked (state 2) after Ba^{2+} enters the channel from the internal or external solution (the figure is drawn with Ba^{2+}

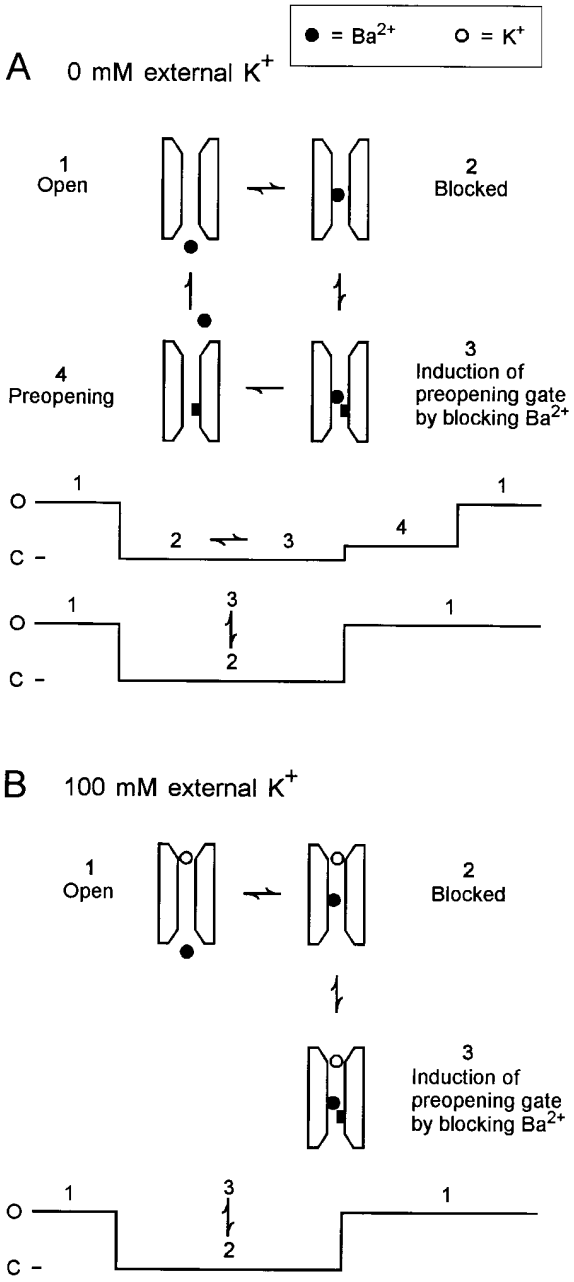

FIGURE 14. Model 2. A cartoon for preopenings when Ba^{2+} induces a preopening gate. (*A*) Generation of preopenings with 0 mM external K^+. Below the model are hypothetical single-channel currents and indicated state transitions for Ba^{2+} blocks with (*top*) and without (*bottom*) preopenings. (*B*) Absence of preopenings with 100 mM external K^+. See text for description of the models.

blocking from the internal solution). Once in state 2, unblocking can occur in either of two ways. Approximately 75% of the time the blocking Ba^{2+} ion dissociates to either the internal or external solution without a preopening (back to state 1). 25% of the time, the blocking Ba^{2+} dissociates to the external solution as the channel passes from state 2 through states 3, 4, and 1. Preclosings are not observed since the channel is blocked to zero current level by the blocking Ba^{2+} ion (state 2) before the preopening gate is induced (state 3).

The reversible transition from state 2 to 3 occurs when the bound Ba^{2+} induces the preopening gate to move and partially occlude the channel so that Ba^{2+} can no longer dissociate to the inside. Ba^{2+} is then forced to dissociate to the outside (state 4). It is state 4 that gives rise to the preopening since the preopening gate partially obstructs the unblocked channel.

After ~0.75 ms in state 4, the preopening gate relaxes and the channel makes the transition from preopening state 4 to the fully open channel in state 1.

With zero external Ba^{2+}, the dissociation of Ba^{2+} to the outside in the transition from state 3 to 4 would be irreversible, since the single Ba^{2+} ion is immediately lost into the external solution. The irreversible arrow from state 3 to 4 is drawn for this condition. With Ba^{2+} outside, the step is potentially reversible, but could appear irreversible since the chance of Ba^{2+} entering and blocking the channel during the 0.75-ms average lifetime of the preopening would be small. After the preopening gate has relaxed in the transition from state 4 to 1, it cannot be ruled out that it spontaneously moves into the pore of the channel for brief periods of time in the absence of Ba^{2+} block, just as liganded receptor channels can open infrequently and for very brief periods of time in the absence of agonist (Jackson, 1986). A binding of a Ba^{2+} when the preopening gate was in the channel would then make the step reversible and produce a preclosing. However, the absence of observed preclosings in the presence of external Ba^{2+} would suggest that such a sequence of steps occurs infrequently, if at all. Below the model in Fig. 14 *A* are hypothetical current records (with state transitions) indicated for Ba^{2+} block with (*top*) and without (*bottom*) a preopening.

Fig. 14 *B* depicts the gating with 100 mM external K^+ (or Rb^+). The external K^+ (or Rb^+) binds to the external lock-in and enhancement sites, blocking the dissociation of Ba^{2+} to the external solution (states 2 and 3). Since Ba^{2+} cannot exit to the external solution, and since the preopening gate must be retracted to allow Ba^{2+} to exit to the internal solution (state 2), no preopenings are seen. Below the model is a hypothetical current record (with state transitions) for Ba^{2+} block when the external lock-in site is occupied.

An alternative explanation for the reduction of the fraction of Ba^{2+} blocks with preopenings in the presence of external K^+, Rb^+, Na^+, or Ba^{2+} is that the external ions act not by preventing Ba^{2+} exit to the external solution, but through an allosteric mechanism to prevent the blocking Ba^{2+} ion from inducing the preopening gate. Although an allosteric inhibition cannot be excluded, the observations of Neyton and Miller (1988*a*,

1988*b*) that these ions inhibit the dissociation of Ba^{2+} to the external solution provide a more parsimonious means to explain the effects of these ions on preventing preopenings.

For the models in Figs. 13 and 14, the binding of K^+ to the external lock-in and/or enhancement sites can prevent the exit of Ba^{2+} to the external solution. On this basis, it might be asked how the channel can carry such large outward K^+ currents in the absence of Ba^{2+} under conditions of high external K^+ when these sites would be occupied. Apparently, K^+ ions bound to the various sites within the channel destabilize the binding of K^+, leading to a rapid exchange of K^+ across the sites and through the channel (Yellen, 1984*a*, 1984*b*; Neyton and Miller, 1988*a*, 1988*b*).

What Drives the Time-irreversible Gating?

The results discussed in the previous sections suggest that preopenings can be observed if the blocking Ba^{2+} ion dissociates (is knocked off) to the external rather than the internal solution. Thus, factors that prevent the knock off of Ba^{2+} to the external solution will decrease the fraction of Ba^{2+} blocks with preopenings. Since permeant as well as impermeant ions can influence the knock off of blocking ions from channels (Armstrong, 1975; Armstrong et al., 1982; Yellen, 1984*a*, 1984*b*; Neyton and Miller, 1988*a*, 1988*b*; Armstrong and Palti, 1991), our experiments do not unequivocally indicate the energy source for the time-irreversible gating. The outward flux of K^+ through the channel in our experiments would act to push the blocking Ba^{2+} ion into the extracellular solution. Decreasing the net outward flux of K^+ by adding external K^+ decreased the fraction of blocks with preopenings, until at 100 mM external K^+, no preopenings were seen. Adding 100 mM of the permeant ion Rb^+ to the extracellular solution in place of the external K^+ had the same effect (Fig. 11), suggesting that the flux of monovalent cations may supply the energy for the time-irreversible gating.

However, 100 mM external Na^+ or 10 mM external Ba^{2+}, two ions with negligible flux through the channel, also decreased the fraction of Ba^{2+} blocks with preopenings (Figs. 12 and 13), although less effectively than 100 mM external K^+ or Rb^+. Thus, it becomes difficult to distinguish whether external K^+ and Rb^+ are having their effects by decreasing the concentration gradient for highly permeant monovalent cations, or by binding to external sites to prevent Ba^{2+} exit (as Na^+ does), or both.

It is also unclear to what extent the electrochemical gradient of Ba^{2+} drives the time-irreversible gating. The observation that preopenings are observed with either inward or outward Ba^{2+} gradients indicates that the Ba^{2+} gradient is not a required energy source for the irreversible subconductance gating. In support of this notion, increasing the concentration of internal Ba^{2+} five orders of magnitude had little effect on the fraction of Ba^{2+} blocks with preopenings (Fig. 5). In contrast, 10 mM external Ba^{2+} decreased the fraction of Ba^{2+} blocks with preopenings (Fig. 12), suggesting that the Ba^{2+} gradient may have some effect on the time-irreversible gating. However, the external Ba^{2+} may have exerted its inhibitory effect by binding to an external site and preventing exit of the blocking Ba^{2+}, rather than through a reversal of the concentration gradient.

While the outward flux of K^+ through the channel is the most likely source of energy to drive the irreversible subconductance gating, further experiments over a wider range of experimental conditions will be required to clarify the contributions of all the various factors, such as external impermeant ions and external Ba^{2+} to the irreversible subconductance gating.

The Fractional Amplitude of the Preopenings Varies with Membrane Potential

Dani and Fox (1991) have discussed three mechanisms that could give reduced conductance levels: alterations in the electrical charge at the vestibules, long lived conformational states, and rapid fluctuations between conformational states of different conductances (Figs. 13 and 14, Models *1* and *2*). There was no indication in our experiments that the preopenings arose from rapid fluctuations between conformational states, because the open channel noise during the preopenings (excluding the gating) typically appeared no greater than that during the closed current level (Figs. 2–6, 10, and 12; compare with Fig. 8 *B* in Blatz and Magleby, 1986, which presents an experimental example of a subconductance state from rapid fluctuation).

Over the 80-mV change in membrane potential from +10 to +90 mV, the fractional conductance of the preopenings increased from 0.24 to 0.39 of the fully open level (Fig. 9). In theory, the models in Figs. 13 and 14 could automatically account for this relative change in conductance if the preopening gate were located deeper in the conducting pore from the inside than the barrier to conductance associated with the fully open channel. The reason for this is that the addition (or elevation) of a second barrier in a conducting pore can change the shape of the current–voltage curve (Hille and Schwarz, 1978; Hille, 1992).

In support of this approach, Schild and Moczydlowski (1994) have used Eyring rate theory to describe the greater effect of voltage on Zn^{2+}-induced subconductance levels for a sodium channel (see below), and we have found that a model based on Poisson-Nernst-Plank theory (Chen et al., 1997) with a preopening-

associated electrostatic barrier near the outer end of the pore can approximate the current–voltage curves in Fig. 9 (our unpublished observations).

Other models are also possible. For example, the changes in voltage itself may alter the position of the preopening gate, changing directly the conductance of the preopening.

Whatever the mechanism of the preopenings, it differs from the mechanism for the subconductance levels observed during normal gating since the subconductance levels did not change their fractional conductance with voltage (Fig. 10). If the subconductance levels entered during normal gating represent partial closure of the gate used for normal gating (Chapman et al., 1997), then the subconductance levels observed during normal gating might be expected to maintain the same fractional conductance with changes in membrane potential as the main conductance level, as was observed, since the subconductance gates during normal gating and the normal gate would be located at the same place in the electric field. On this basis, since K^+ channels typically have a gate at the interior side of the channel (Armstrong, 1971; Miller et al., 1987; Miller, 1987; Holmgren et al., 1997), then the gate for the subconductance levels during normal gating would be located at the interior side as well. The preopening gate could then be located deeper in the pore of the channel from the inside.

Similar to the preopenings, but unlike the normal subconductance levels that we observed, a subconductance level with a fractional conductance that depends on membrane potential has been described for a large conductance K^+ channel from the alga *Chara corallina* (Tyerman et al., 1992). The subconductance levels in *C. corallina* were not associated with asymmetric gating.

Subconductance Levels Associated with the Binding of Divalent Metal Cations in Other Channels

Schild and Moczydlowski (1994) found that the association of Zn^{2+} with a cystine residue in the outer vestibule of cardiac Na^+ channels led to a subconductance level that displayed a weak outward rectification, similar to what we observed for preopenings associated with the Ba^{2+} block of BK channels. They suggest that the binding of Zn^{2+} in the external vestibule near the pore at a site very close to a high affinity Na^+-binding site leads to Zn^{2+}–Na^+ repulsion, which decreases the flux of Na^+ through the channel. The mechanism in Fig. 13 (Model 1) for the Ba^{2+}-induced subconductance level is thus similar to the mechanism of Schild and Moczydlowski (1994) for the Zn^{2+}-induced subconductance level, except that we have located the Ba^{2+}-binding site for the subconductance level deeper into the pore, since this Ba^{2+}-subconductance site was not readily accessible by external Ba^{2+}.

Premkumar and Auerbach (1996) have also found a subconductance level associated with the binding of a divalent metal ion. They found that the binding of Ca^{2+} near the outer entrance of the pore of NMDA receptors reduced the conductance by 93%.

In contrast to our observations on the Ba^{2+} subconductance level, neither the Zn^{2+}- nor Ca^{2+}-induced subconductance levels were reported to be associated with irreversible gating.

Asymmetric Subconductance Gating in Other Channels

Hamill and Sakmann (1981) recorded inward single-channel currents through ACh receptors. In one experiment where a total of 809 discrete events were analyzed, 100 events demonstrated gating to a subconductance level. Transitions similar to preclosings (closed level–main level–subconductance level–closed level) could be observed, whereas transitions similar to preopenings (closed level–subconductance level–main level) were not observed. The causative factor for the subconductance gating was not established.

Trautmann (1982) found that subconductance levels were observed when ACh receptors were activated by 20 μM curare, and that the frequency of the subconductance levels increased with the concentration of curare. Transitions similar to preclosings occurred about three times more frequently than transitions similar to preopenings.

Both cloned and native NMDA receptors display asymmetry in gating, with transitions from the main level to the subconductance level (similar to our preclosings) being ~60% more frequent than transitions from the subconductance to the main level (Cull-Candy and Usowicz, 1987; Wyllie et al., 1997). Cull-Candy and Usowicz (1987) ruled out the potential gradient as the driving force.

Schneggenburger and Ascher (1997) have found a gating asymmetry in the transitions among the closed, main, and subconductance levels for a mutant NMDA receptor. The direction and level of asymmetry could be accounted for by assuming that ions bound to a site in the permeation pathway influenced the gating, and that the site was accessible to the internal cations in the closed state.

Chloride channels from *Torpedo* gate as if they are formed by two protochannels (Richard and Miller, 1990). The single channel records have an inactivated nonconducting state, a brief closed state, and two conducting states corresponding to one or two open protochannels. The channel enters the inactivated state preferentially from one open protochannel and leaves the inactivated state preferentially to two open protochannels, with the asymmetry ratio in gating increasing from ~1.5 to 15 as the membrane potential was changed from −20 to −80 mV. The asymmetric gating

is driven by the electrochemical gradient for Cl^-, with a bound Cl^- providing the gating charge (Chen and Miller, 1996).

The characteristics of the asymmetric gating differed among these various studies. The subconductance gating was essentially one way in our study, whereas in the other studies (excluding the one by Hamill and Sakmann, 1981) there was a preferential asymmetry in the gating. Only (essentially) preopenings were observed in our study, compared with only preclosings in the study of Hamill and Sakmann (1981). Both preopenings and preclosings, with a preference for preclosings, were observed in the studies of Trautman (1982), Cull-Candy and Usowicz (1987), and Wyllie et al. (1997). Schneggenburger and Ascher (1997) observed both preopenings and preclosings, with the preference dependent on the ionic conditions.

Although the characteristics of the asymmetric gating differed among the various studies, the mechanisms (when examined) appeared similar in that an ion binding in the permeation pathway influenced the gating of the channel. In our study, a blocking Ba^{2+} ion binds to the conduction pathway and induces the asymmetric gating either directly (Fig. 13, *Model 1*) or indirectly (Fig. 14, *Model 2*), while in the other studies (when examined) a highly permeant ion binds and induces the asymmetric gating.

We thank Dr. W. Nonner for assistance with applying Poisson-Nernst-Planck theory to calculate ionic currents through a channel with two effective barriers.

This work was supported in part by grants from the National Institutes of Health (AR-32805, NS-30584, and NS-007044) and the Muscular Dystrophy Association.

Original version received 11 August 1997 and accepted version received 18 November 1997.

REFERENCES

Armstrong, C.M. 1971. Interaction of tetraethylammonium ion derivatives with the potassium channel of giant axons. *J. Gen. Physiol.* 58:413–437.

Armstrong, C.M. 1975. Potassium pores of nerve and muscle membranes. *In* Membranes. Volume 3. G. Eisenman, editor. Marcel Dekker, Inc. New York. 325–357.

Armstrong, C.M., and S.R. Taylor. 1980. Interaction of barium ions with potassium channels in squid giant axons. *J. Gen. Physiol.* 30: 473–488.

Armstrong, C.M., and Y. Palti. 1991. Potassium channel block by internal calcium and strontium. *J. Gen. Physiol.* 97:627–638.

Armstrong, C.M., R.P. Swenson, and S.R. Taylor. 1982. Block of squid axon K channels by internally and externally applied barium ions. *J. Gen. Physiol.* 80:663–682.

Barrett, J.N., K.L. Magleby, and B.S. Pallotta. 1982. Properties of single calcium-activated potassium channels in cultured rat muscle. *J. Physiol. (Camb.).* 331:211–230.

Baukrowitz, T., and G. Yellen. 1996. Use-dependent blockers and exit rate of the last ion from the multi-ion pore of a K^+ channel. *Science.* 271:653–656.

Benham, C.D., T.B. Bolton, R.J. Lang, and T. Takewaki. 1985. The mechanism of action of Ba^{2+} and TEA on single Ca^{2+}-activated K^+-channels in arterial and intestinal smooth muscle cell membranes. *Pflügers Arch.* 403:120–127.

Bello, R.A., and K.L. Magleby. 1996. Differential effect of voltage on the open channel conductance level and the Ba^{2+}-induced subconductance level in Ca^{2+}-activated K^+ (BK) channels from rat skeletal muscle. *Biophys. J.* 70:*A*192.

Blatz, A.L., and K.L. Magleby. 1984. Ion conductance and selectivity of single calcium-activated potassium channels in cultured rat muscle. *J. Gen. Physiol.* 84:1–23.

Blatz, A.L., and K.L. Magleby. 1986. Quantitative description of three modes of activity of fast chloride channels from rat skeletal muscle. *J. Physiol. (Camb.).* 378:141–174.

Chapman, M.L., H.M.A. VanDongen, and A.M.J. VanDongen. 1997. Activation-dependent subconductance levels in the drk1 K channel suggest a subunit basis for ion permeation and gating. *J. Gen. Physiol.* 72:708–719.

Chen, D., J. Lear, and B. Eisenberg. 1997. Permeation through an open channel: Poisson-Nernst-Plank theory of a synthetic ionic channel. *Biophys. J.* 72:97–116.

Chen, T.-Y., and C. Miller. 1996. Nonequilibrium gating and voltage dependence of the ClC-0 Cl− channel. *J. Gen. Physiol.* 108: 237–250.

Colquhoun, D., and A.G. Hawkes. 1983. The principles of the stochastic interpretation of ion channel mechanisms. *In* Single Channel Recording. B. Sakmann and E. Neher, editors. Plenum Publishing Corp., New York. 135–175.

Cull-Candy, S.G., and M.M. Usowicz. 1987. Multiple-conductance channels activated by excitatory amino acids in cerebellar neurons. *Nature.* 325:525–528.

Dani, J.A., and J.A. Fox. 1991. Examination of subconductance levels arising from a single ion channel. *J. Theor. Biol.* 153:401–423.

Diaz, F., M. Wallner, E. Stefani, L. Toro, and R. Latorre. 1996. Interaction of internal Ba^{2+} with a cloned Ca^{2+}-dependent K^+ (h*slo*) channel from smooth muscle. *J. Gen. Physiol.* 107:399–407.

Ferguson, W.B. 1991. Competitive Mg^{2+} block of a large-conductance Ca^{2+}-activated K^+ channel in rat skeletal muscle: Ca^{2+}, Sr^{2+}, and Ni^{2+} also block. *J. Gen. Physiol.* 98:163–181.

Ferguson, W.B., R.A. Bello, L. Song, and K.L. Magleby. 1994. Barium-induced asymmetric occurrence of a subconductance level in BK channels from rat skeletal muscle. *Biophys. J.* 66:*A*208.

Ferguson, W.B., O.B. McManus, and K.L. Magleby. 1993. Opening and closing transitions for BK channels often occur in two steps via sojourns through a brief lifetime subconductance state. *Biophys. J.* 65:702–714.

Hamill, O.P., A. Marty, E. Neher, B. Sakmann, and F.J. Sigworth. 1981. Improved patch clamp techniques for high-resolution current recording from cells and cell-free membrane patches. *Pflügers Arch.* 391:85–100.

Hamill, O.P., and B. Sakmann. 1981. Multiple conductance states of single acetylcholine receptor channels in embryonic muscle

cells. *Nature.* 294:462–464.
Hille, B. 1992. Ionic Channels of Excitable Membranes. Sinauer Associates, Inc., Sunderland, MA. 607 pp.
Hille, B., and W. Schwarz. 1978. Potassium channels as multi-ion single-file pores. *J. Gen. Physiol.* 72:409–442.
Holmgren, M., P.L. Smith, and G. Yellen. 1997. Trapping of organic blockers by closing of voltage-dependent K^+ channels. Evidence for a trap door mechanism of activation gating. *J. Gen Physiol.* 109:527–535.
Hurst, R.S., R. Latorre, L. Toro, and E. Stefani. 1995. External barium block of *Shaker* potassium channels: evidence for two binding sites. *J. Gen Physiol.* 106:1069–1087.
Jackson, M.B. 1986. Kinetics of unliganded acetylcholine receptor channel gating. *Biophys. J.* 49:663–672.
Kijima, S., and H. Kijima. 1987. Statistical analysis of channel current from a membrane patch. I. Some stochastic properties of ion channels or molecular systems in equilibrium. *J. Theor. Biol.* 128:423–434.
Kirber, M.T., J.J. Singer, J.V. Walsh, Jr., M.S. Fuller, and R.A. Peura. 1985. Possible forms for dwell-time histograms from single-channel current records. *J. Theor. Biol.* 116:111–126.
Lauger, P. 1983. Conformational transitions of ionic channels. *In* Single Channel Recording. B. Sakmann and E. Neher, editors. 177–189. Plenum Publishing Corp., New York. 177–189.
Lauger, P. 1985. Ionic channels with conformational substates. *Biophys. J.* 47:581–591.
Lucchesi, K.J., and E. Moczydlowski. 1991. On the interaction of bovine pancreatic trypsin inhibitor with maxi Ca^{2+}-activated K^+ channels: a model system for analysis of peptide-induced subconductance states. *J. Gen. Physiol.* 97:1295–1319.
McManus, O.B., A.L. Blatz, and K.L. Magleby. 1987. Sampling, log binning, fitting, and plotting durations of open and shut intervals from single channels and the effect of noise. *Pflügers Arch.* 410:530–553.
McManus, O.B., and K.L. Magleby. 1988. Kinetic states and modes of single large-conductance calcium-activated potassium channels in cultured rat skeletal muscle. *J. Physiol. (Camb.).* 402:79–120.
McManus, O.B., and K.L. Magleby. 1989. Kinetic time constants independent of previous single channel activity suggest Markov gating for a large conductance Ca-activated K channel. *J. Gen. Physiol.* 94:1037–1070.
Miller, C. 1987. Trapping single ions inside single ion channels. *Biophys. J.* 52:123–126.
Miller, C., R. Latorre, and I. Reisin. 1987. Coupling of voltage-dependent gating and Ba^{++} block in the high conductance, Ca^{2+}-activated K^+ channel. *J. Gen. Physiol.* 90:427–449.
Moczydlowski, E., and R. Latorre. 1983. Gating kinetics of Ca^{2+}-activated K^+ channels from rat muscle incorporated into planar lipid bilayers. Evidence for two voltage-dependent Ca^{2+}-binding reactions. *J. Gen Physiol.* 82:511–542.
Neyton, J., and C. Miller. 1988*a*. Potassium blocks barium permeation through a calcium-activated potassium channel. *J. Gen. Physiol.* 92:549–567.
Neyton, J., and C. Miller. 1988*b*. Discrete Ba^{2+} block as a probe of ion occupancy and pore structure in the high-conductance Ca^{2+}-activated K^+ channel. *J. Gen. Physiol.* 92:569–586.
Neyton, J., and M. Pelleschi. 1991. Multi-ion occupancy alters gating in high-conductance, Ca^{2+}-activated K channels. *J. Gen. Physiol.* 97:641–665.
Oberhauser, A., O. Alvarez, and R. Latorre. 1988. Activation by divalent cations of a Ca^{2+}-activated K^+ channel from skeletal muscle membrane. *J. Gen. Physiol.* 92:67–86.
Premkumar, L.S., and A. Auerbach. 1996. Identification of a high affinity divalent cation binding site near the entrance of the NMDA receptor channel. *Neuron.* 16:869–880.
Richard, E.A., and C. Miller. 1990. Steady-state coupling of ion-channel conformations to a transmembrane ion gradient. *Nature.* 247:1208–1210.
Rothberg, B.S., R.A. Bello, L. Song, and K.L. Magleby. 1996. High Ca^{2+} concentrations induce a low activity mode and reveal Ca^{2+}-independent long shut intervals in BK channels from rat muscle. *J. Physiol. (Camb.).* 493:673–689.
Schild, L., and E. Moczydlowski. 1994. Permeation of Na^+ through open and Zn^{2+}-occupied conductance states of cardiac sodium channels modified by batrachotoxin: exploring ion–ion interactions in a multi-ion channel. *Biophys. J.* 66:654–666.
Schneggenburger, R., and P. Ascher. 1997. Coupling of permeation and gating in an NMDA-channel pore mutant. *Neuron.* 18:167–177.
Slesinger, P.A., Y.N. Jan, and L.Y. Jan. 1993. The S4-S5 loop contributes to the ion-selective pore of potassium channels. *Neuron.* 11:739–749.
Sohma, Y., A. Harris, C.J.C. Wardle, B.E. Argent, and M.A. Gray. 1996. Two barium binding sites on a maxi K^+ channel from human vas deferens epithelial cells. *Biophys. J.* 70:1316–1325.
Song, L., and K.L. Magleby. 1994. Testing for microscopic reversibility in the gating of maxi K^+ channels using two-dimensional dwell-time distributions. *Biophys. J.* 67:91–104.
Steinberg, I.Z., 1987*a*. Frequencies of paired open-closed durations of ion channel. *Biophys. J.* 52:47–55.
Steinberg, I.Z. 1987*b*. Relationship between statistical properties of single ionic channel recordings and the thermodynamics state of the channels. *J. Theor. Biol.* 124:71–87.
Stockbridge, L.L., and A.S. French. 1989. Characterization of a calcium-activated potassium channel in human fibroblasts. *Can. J. Physiol. Pharmacol.* 67:1300–1307.
Stockbridge, L.L., A.S. French, and S.F.P. Man. 1991. Subconductance states in calcium-activated potassium channels from canine airway smooth muscle. *Biochim. Biophys. Acta.* 1064:212–218.
Taglialatela, M., J.A. Drewe, and A.M. Brown. 1993. Barium blockade of a clonal potassium channel and its regulation by a critical pore residue. *Mol. Pharmacol.* 44:180–190.
Trautmann, A. 1982. Curare can open and block ionic channels associated with cholinergic receptors. *Nature.* 298:272–275.
Tyerman, S.D., B.R. Terry, and G.P. Findlay. 1992. Multiple conductances in the large K^+ channel from Chara coralina shown by a transient analysis method. *Biophys. J.* 61:736–749.
Vergara, C., and R. Latorre. 1983. Kinetics of Ca^{2+}-activated K^+ channels from rabbit muscle incorporated into planar bilayers. *J. Gen. Physiol.* 82:543–568.
Wyllie, D.J.A., P. Be'he', M. Nassar, R. Schoepfer, and D. Colquhoun. 1996. Single-channel currents from recombinant NMDA NR1a/NR2D receptors expressed in *Xenopus* oocytes. *J. Gen. Physiol.* 263:1079–1086.
Yellen, G. 1984*a*. Ionic permeation and blockade in Ca^{2+}-activated K^+ channels of bovine chromaffin cells. *J. Gen. Physiol.* 84:157–186.
Yellen, G. 1984*b*. Relief of Na^+ block of Ca^{2+}-activated K^+ channels by external cations. *J. Gen. Physiol.* 84:187–199.